

***N*-demethylation of Alkaloids Using Nanoscale Zero Valent Iron**

By

Jon Kyle Awalt

A Thesis Submitted to

Saint Mary's University, Halifax, Nova Scotia

in Partial Fulfillment of the Requirements for

the Degree of Bachelor of Science

with Honours in Chemistry.

April, 2016, Halifax, Nova Scotia

Copyright Jon Kyle Awalt, 2016, All Rights Reserved.

This work may not be reproduced in whole or in part without the

written permission of the author.

Certification

N-demethylation of Alkaloids Using Nanoscale Zero Valent Iron

I hereby certify that this thesis was carried out by Jon Kyle Awalt in partial fulfillment for the requirements of the Degree of Bachelor of Science, Honours in Chemistry at Saint Mary's University. I certify that this is truly original work carried out by Jon Kyle Awalt.

Supervisor and Chairperson of the Chemistry Department:

Dr. Robert D. Singer

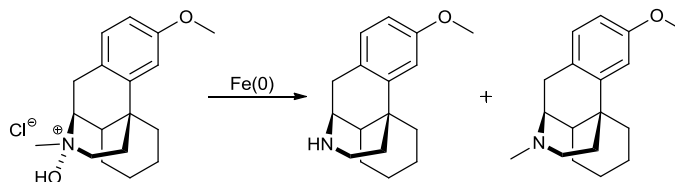
Date: April 21, 2016

Abstract

N-demethylation of Alkaloids Using Nanoscale Zero Valent Iron

By Jon Kyle Awalt

The *N*-demethylation of naturally occurring opiate compounds is a necessary step in the synthesis of many pseudo-opioid pharmaceuticals. Such drugs have gained recent media attention in the fight against opiate addiction; hence, the ability to synthesize them efficiently is important. This work aims to improve the *N*-demethylation of alkaloid precursors through the use of zero valent nanoscale iron in a modified Polonovski reaction. Initial studies performed on dextromethorphan indicate that yields of the demethylated product using a 10 mol % loading of zero valent nanoscale iron are comparable to those achieved by using a stoichiometric amount of commercially available iron (0) dust.¹ The preparation of zero valent nanoscale iron particles and their use in the *N*-demethylation of dextromethorphan will be described.



1

Gaik B. Kok *et al.* J. Org. Chem. 2010, 75, 4806–4811

Submitted _____

Acknowledgements

Firstly I would like to thank my supervisor, Dr. Robert Singer, for providing me with the opportunity to pursue this research and for his support and guidance throughout the process. Not only did he offer advice and encouragement, but also the freedom which enabled me to learn important lessons on my own. Special thanks also to Bitu Hurisso, who was always willing to take time away from his own work to answer my questions and provide me with any assistance I needed, and Andrew Watson, who showed me the ropes during my initial few weeks in the lab.

I would also like to thank Darlene Goucher, Alyssa Doué and Elizabeth McLeod for providing continuous technical support in the lab, Patricia Granados for instrumental training and providing mass spectrometry and elemental analysis characterization, Xiang Yang for providing SEM analysis, and the Brosseau group for their guidance and materials with regards to nanoparticle synthesis and characterization.

Lastly I would like to thank my family, friends, and the entire chemistry department at Saint Mary's, without whom my experience over the past year would not have been as satisfying or as much fun.

Table of Contents

1. Introduction.....	1
1.1. <i>N</i> -demethylation of Alkaloids	1
1.1.1. Introduction to Alkaloids and <i>N</i> -demethylation	1
1.1.2. History of <i>N</i> -demethylation Reactions.....	2
1.1.3. The Polonovski Reaction	5
1.2. Nanoscale Zero Valent Iron	7
1.2.1. Introduction to Nanoscale Heterogeneous Catalysis	7
1.2.2. Heterogeneous Catalysis with Nanoscale Zero Valent Iron	9
1.2.3. Preparation of Nanoscale Zero Valent Iron	10
1.2.4. Relative Reactivity of Nanoscale Zero Valent Iron	11
1.3. An Opiate Model Compound and the Current Work	12
2. Results and Discussion	12
2.1. Preparation and Characterization of Substrates	12
2.2. Preparation and Characterization of Nanoscale Zero Valent Iron	21
2.3. <i>N</i> -demethylation Reactions	24
3. Conclusion	32
4. Future Directions	32
5. Experimental	34

5.1.	General Methods	34
5.2.	Synthesis of <i>N</i> -oxide Hydrochloride salts	35
5.2.1.	Synthesis of <i>N</i> -methylpiperidine <i>N</i> -oxide Hydrochloride	35
5.2.2.	Synthesis of <i>N</i> -methylpyrrolidine <i>N</i> -oxide Hydrochloride.....	36
5.2.3.	Synthesis of Dextromethorphan <i>N</i> -oxide Hydrochloride.....	37
5.3.	Preparation of Nanoscale Zero Valent Iron.....	38
5.3.1.	Preparation of Nanoscale Zero Valent Iron for Immediate Use	38
5.3.2.	Preparation of nZVI for Storage	39
5.4.	<i>N</i> -demethylation of Dextromethorphan <i>N</i> -oxide Hydrochloride	39
5.4.1.	<i>N</i> -demethylation via Iron(0) Dust – General Procedure	39
5.4.2.	<i>N</i> -demethylation <i>via</i> Nanoscale Zero Valent Iron	41
6.	References	42

List of Figures	Page
Figure 1. The naturally occurring opiates thebaine, 1 , codeine, 2 , oripavine, 3 , and morphine, 4 .	1
Figure 2. <i>N</i> -demethylation of morphine, 4 , to normorphine, 5 .	2
Figure 3. Mechanism of the von Braun Reaction	3
Figure 4. Structure of diethyl azodicarboxylate	4
Figure 5. Mechanism of photolytic <i>N</i> -demethylation	4
Figure 6. <i>N</i> -demethylation via the Polonovski Reaction	5
Figure 7. Proposed mechanism of the nonclassical Polonovski reaction	6
Figure 8. Web of Science number of publications found for query “nanoparticle catalysts”, 1997-2016	9
Figure 9. Reduction of an iron salt in aqueous media by sodium borohydride	11
Figure 10. Structures of tertiary methylamine substrates 17 , 18 , 19 , 20	13
Figure 11. Proposed synthesis of substrate <i>N</i> -oxide derivatives 21 , 22 , 23 , 26	14
Figure 12. ¹ H-NMR spectra of <i>N</i> -methylpiperidine <i>N</i> -oxide hydrochloride, 21 , with peak assignments	15
Figure 13. ¹ H-NMR spectra of <i>N</i> -methylpyrrolidine <i>N</i> -oxide hydrochloride, 22 , with peak assignments	16
Figure 14. ¹ H-NMR spectra of DXM <i>N</i> -oxide hydrochloride, 26 , with peak assignments	19
Figure 15. ¹ H-NMR COSY spectra of DXM <i>N</i> -oxide hydrochloride, 26	20
Figure 16. SEM image of lab-synthesized nZVI, 500 nm scale	22
Figure 17. SEM image of lab-synthesized nZVI, 1 μm scale	23
Figure 18. SEM image of iron(0) dust	24
Figure 19. Proposed synthetic pathway of <i>N</i> -nordextromethorphan, 27	25
Figure 20. Comparison between ¹ H-NMR spectra of DXM-HBr, 20 , DXM <i>N</i> -oxide HCl, 26 , and <i>N</i> -norDXM, 27 (aromatic regions removed for size)	31
Figure 21. Synthesis of <i>N</i> -methylpiperidine <i>N</i> -oxide hydrochloride, 21	35
Figure 22. Synthesis of <i>N</i> -methylpyrrolidine <i>N</i> -oxide hydrochloride, 22	36
Figure 23. Synthesis of DXM <i>N</i> -oxide hydrochloride, 26	37
Figure 24. Synthesis of <i>N</i> -norDXM, 27	39

List of Tables	Page
Table 1. Results of a nonclassical Polonovski reaction using an iron(0) activating agent	7
Table 2. Results of <i>N</i> -demethylation of DXM in isopropanol at room temperature with reduced reaction time	26
Table 3. Results of <i>N</i> -demethylation of DXM in chloroform at room temperature with reduced reaction time	27
Table 4. Results of <i>N</i> -demethylation of DXM in methanol at room temperature with reduced reaction time	28
Table 5. Results of <i>N</i> -demethylation of DXM in various solvents using less than a stoichiometric amount of activating species	29
Table 6. Results of <i>N</i> -demethylation of DXM in isopropanol at room temperature with further reduced reaction time	30

Abbreviations

DEAD	Diethyl azodicarboxylate
DCA	9,10-dicyanoanthracene
TPP	5,10,15,20-tetraphenyl-21 <i>H</i> ,23 <i>H</i> -porphyrin
CO	Carbon monoxide
CO ₂	Carbon dioxide
nm	Nanometer
nZVI	Nanoscale zero valent iron
E. coli	Escherichia coli
NaBH ₄	Sodium borohydride
Fe ₃ O ₄	Magnetite
FeO(OH)	Goethite
DBDE	Decabrominated diphenyl ether
mZVI	Microscale zero valent iron
DXM	Dextromethorphan
GC-FID	Gas chromatography-flame ionization detector
EA	Elemental analysis
ESI-MS	Electrospray ionization-mass spectrometry
mCPBA	Metachloroperoxybenzoic acid
¹ H-NMR	¹ Hydrogen-nuclear magnetic spectroscopy
¹³ C-NMR	¹³ Carbon-nuclear magnetic spectroscopy
COSY	Correlation spectroscopy
SEM	Scanning electron microscopy
CEAR	Center for Environmental Analysis and Remediation
CHN	Carbon/Hydrogen/Nitrogen
ATR	Attenuated Total Reflection
RPM	Revolutions per minute
MP	Melting point
RT	Room temperature

1. Introduction

1.1. N-demethylation of Alkaloids

1.1.1. Introduction to Alkaloids and N-demethylation

The term “alkaloid” refers to any naturally occurring compound containing at least one basic nitrogen atom.¹ Opiate compounds are a subset of molecules which are classified as alkaloids and are present in the plant *papaver somniferum*; better known as the poppy plant.² Examples of these compounds include thebaine, **1**, codeine, **2**, oripavine, **3** and morphine, **4** (Figure 1). As with many alkaloids, these examples contain a heterocyclic, basic nitrogen atom. When this nitrogen atom is bonded to a methyl group, making it tertiary, an N-demethylation reaction breaks the N-CH₃ bond, changing the substrate into a secondary amine (Figure 2).

Figure 1. The naturally occurring opiates thebaine, **1**, codeine, **2**, oripavine, **3**, and morphine, **4**.

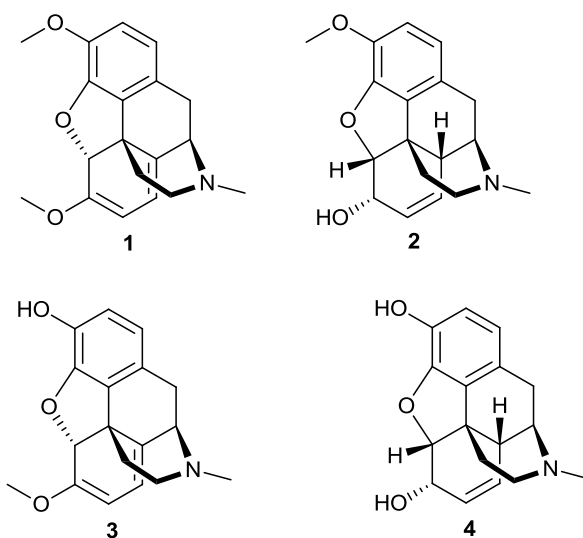
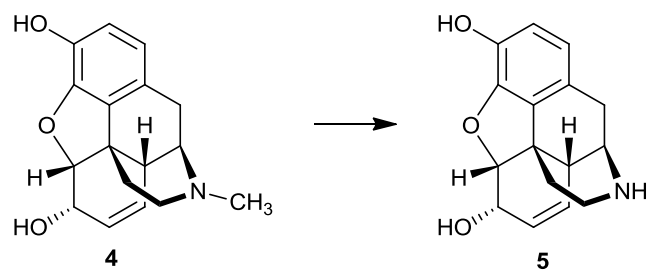


Figure 2. *N*-demethylation of morphine, **4**, to normorphine, **5**.

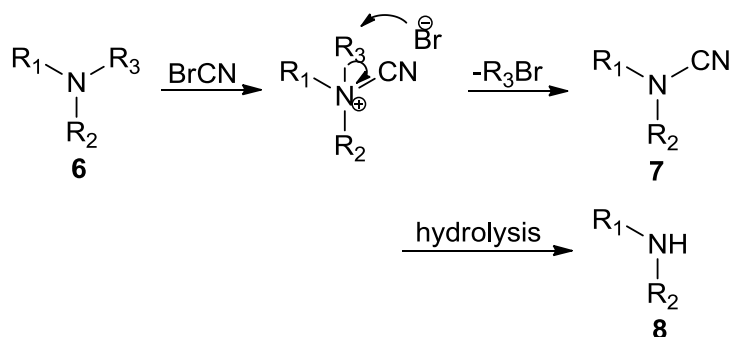


N-demethylation reactions have been studied since as far back as the 1950s. Miller and Anderson in 1954,³ Axelrod in 1956,⁴ Cochin and Axelrod in 1957,⁵ and Ellison *et al.* in 1961⁶ are examples of scientists studying the effects and mechanism of enzymatic *N*-demethylation of morphine in the liver. The conclusions of Axelrod in his 1956 study were that a lack of *N*-demethylation performed in the liver was responsible for tolerance to morphine in rats. He also discovered that rats treated with both morphine and normorphine, **5**, showed less of a response to the biological effects of morphine than rats treated with morphine alone.⁴

1.1.2. History of *N*-demethylation Reactions

There are various applications of opiate alkaloid *N*-demethylations including the conversion of thebaine into the pharmaceutical opioid naloxone⁷ and oripavine into the pharmaceutical opioid buprenorphine.⁸ The von Braun reaction, named after Julius von Braun (1875-1940), is a method of *N*-demethylating tertiary amines and was first reported in 1900.⁹ Figure 3 shows the synthetic pathway of this method which involves the treatment of the starting tertiary amine **6** with cyanogen bromide, resulting in the formation of a disubstituted cyanamide, **7**, which, *via* acid¹⁰ or base¹¹ hydrolysis, yields the secondary amine, **8**.

Figure 3. Mechanism of the von Braun Reaction⁵¹

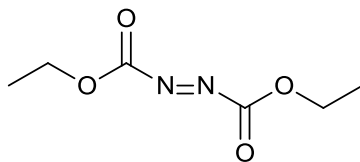


While the von Braun reaction is a straight forward *N*-demethylation technique that gives good results, it also utilizes an extremely toxic reagent; cyanogen bromide is toxic to humans and aquatic life.¹²

In 1967 a patent was filed in the United States describing a process to *N*-demethylate the naturally occurring opiate thebaine.¹³ A reaction mixture of thebaine, diethyl azodicarboxylate and an organic solvent is refluxed for 1-6 hours, giving *N*-(1,2-dicarbethoxyhydrazinylmethyl)thebaine, followed by hydrolysis by ammonium chloride to yield approximately 50% of the *N*-northebaine hydrochloride product. Diethyl azodicarboxylate (DEAD, Figure 4) has also been used to *N*-demethylate a complex semisynthetic macrocyclic ketolide, providing the desired product in 82% yield where previous *N*-demethylation methods had been unsuccessful.

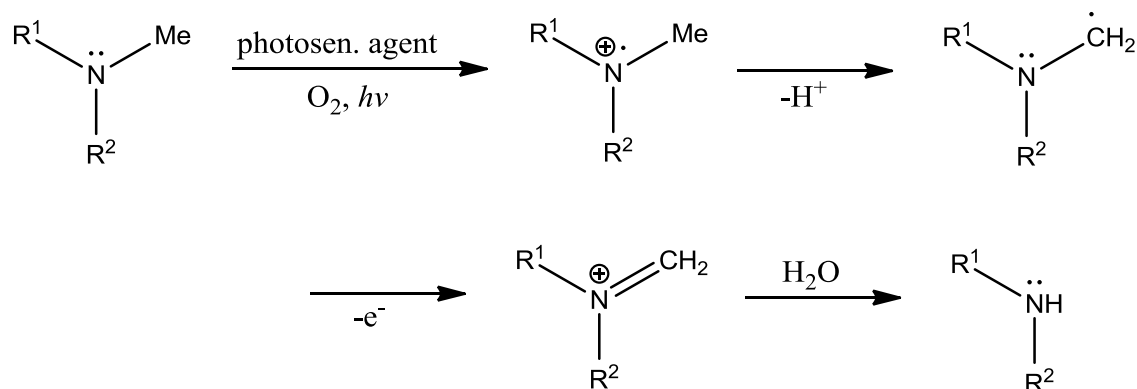
Photooxidation has been utilized for the *N*-demethylation of alkaloids and was first reported in 1989 by Santamaria *et al.*¹⁴ and later in 2001 by Ripper *et al.*¹⁵ Photosensitizing agents such as 2,7-di-methyl-2,7-diazapyrene-2,7-dium bis(tetrafluoroborate)

Figure 4. Structure of diethyl azodicarboxylate



(DAP²⁺[BF₄⁻]₂) 9,10-dicyanoanthracene (DCA), 4,5,6,7-tetrachloro-2',4',5',7'-tetraiodofluorescein (Rose Bengal), and 5,10,15,20-tetraphenyl-21*H*,23*H*-porphyrin (TPP) have been used to afford the *N*-demethylation of various tropane alkaloids in high yields. In addition, it was found that the inclusion of a salt, such as lithium perchlorate, in the reaction mixture can vastly improve yields, which in some cases reach as high as 100%.¹⁶ Application of this method to opiate alkaloids has also had success. When Rose Bengal is used as the photosensitizing agent codeine can be converted to *N*-norcodeine in a 72% yield.¹⁷ It is thought that the reaction proceeds *via* an initial electron transfer to the photosensitizer from the tertiary nitrogen giving an α -amino radical which then forms an iminium ion that, upon hydrolysis, forms the corresponding secondary amine (Figure 5).¹⁶

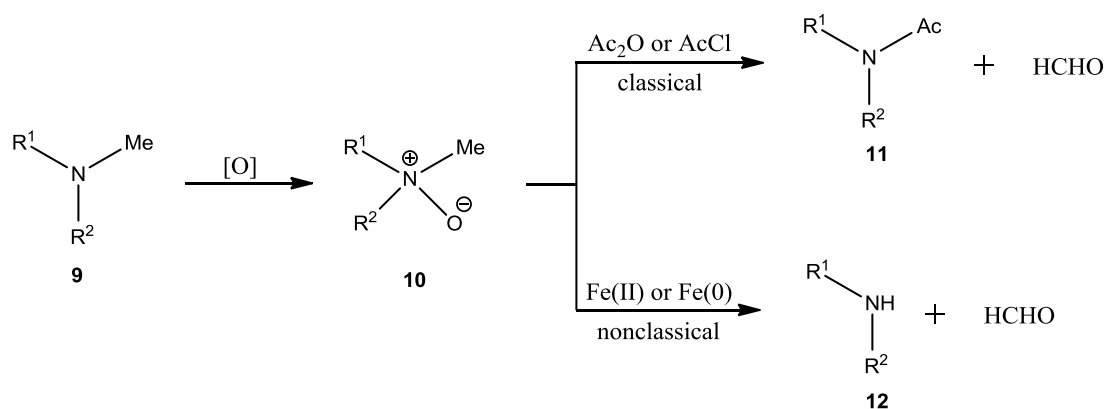
Figure 5. Mechanism of photolytic *N*-demethylation¹⁶



1.1.3. The Polonovski Reaction

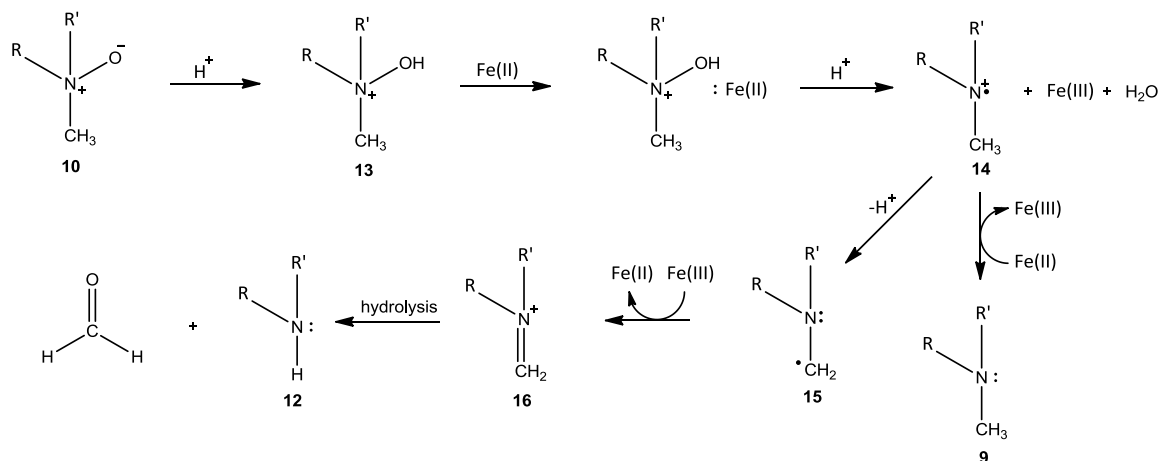
The Polonovski reaction, first reported in 1927 by Max and Michel Polonovski,¹⁸ has been used to *N*-demethylate tertiary amines. In this transformation, treatment of a tertiary amine *N*-oxide with acetic anhydride or acetyl chloride induces a rearrangement leading to the cleavage of one alkyl group from the nitrogen atom. A wide range of *N*-methyl alkaloids have been successfully demethylated using this approach. In 2003, McCamley *et al.* cited the high expense of the reagents employed in this “classical” version of the Polonovski reaction in their paper entitled, “Efficient *N*-Demethylation of Opiate Alkaloids Using a Modified Nonclassical Polonovski Reaction.” They reported an iron(II) species was used instead of the classical chloroformate esters. Figure 6 shows the reaction scheme of both versions. In each, the tertiary methylamine, **9**, is treated with an oxidizing agent to produce the *N*-oxide derivative, **10**. In the classical method the *N*-oxide is reacted with the activating species to form an *N,N*-dialkylacetamide, **11**, which undergoes hydrolysis to form a secondary amine. In the nonclassical method the secondary amine, **12**, is formed directly. Formaldehyde is formed in each case.

Figure 6. *N*-demethylation *via* the Polonovski Reaction⁵²



In 2003 McCamley, Ripper, Singer, and Scammells proposed a mechanism for their nonclassical Polonovski reaction (Figure 7).¹⁹ In this mechanism, after protonation of the *N*-oxide, **10**, iron(II) undergoes a one-electron reduction which results in cleavage of the N-O bond of the protonated *N*-oxide, **13**, and formation of an aminium radical cation **14**. The radical cation loses an α -proton and undergoes an electron reorganization to form a carbon centered radical, **15**. It is this step which affords the selectivity for demethylation as opposed to a more general dealkylation. The α -proton lost is preferentially from the methyl group due to a relative lack of steric hindrance. **15** is then oxidized by iron(III) to form an iminium ion, **16**. Hydrolysis then affords the secondary amine, **11**. Because both iron(II) and iron(III) are present in the reaction mixture, the aminium radical cation can be reduced instead of oxidized, and when this occurs the parent form of the original substrate, **9**, is formed as a by-product. This mechanism represents an iron(II)/iron(III) redox system.

Figure 7. Proposed mechanism of the nonclassical Polonovski reaction¹⁹



The modified, nonclassical Polonovski reaction represents an environmentally green alternative to the methods described previously because iron is used as the activating agent and alcohols are used as solvents. It also provides relatively high yields of the demethylated product across a wide variety of opiate and pseudo-opiate alkaloids.

In 2010, after a member of Scammells' research team accidentally demethylated a substrate simply by leaving a micro spatula submerged in a solution, Kok *et al.* set out to show that an iron(0) activating species was a viable alternative to iron(II).²⁰ Some of their findings are presented in Table 1.

Table 1. Results of a nonclassical Polonovski reaction using an iron(0) activating agent²⁰

Substrate ^a	Iron(0) equiv.	Solvent	Time (h)	Temp. (°C)	Isolated Yield (%) ^b
Morphine	0.5	<i>i</i> -PrOH	24	40	58
CME ^c	1.0	<i>i</i> -PrOH	48	RT	88
Thebaine	1.3	<i>i</i> -PrOH	48	RT-50 ^d	77
Oripavine	2.0	<i>i</i> -PrOH	48	40-60 ^e	40

^aReaction performed on the *N*-oxide hydrochloride salt of the substrates listed. ^bIsolated yield of the demethylated derivative of the substrates listed. ^cCME stands for Codeine Methyl Ether. ^dReaction mixture was stirred at room temperature for 24 hours followed by 50 °C for 24 hours ^eReaction mixture was stirred at 40 °C for 24 hours followed by 60 °C for 24 hours.

1.2. Nanoscale Zero Valent Iron

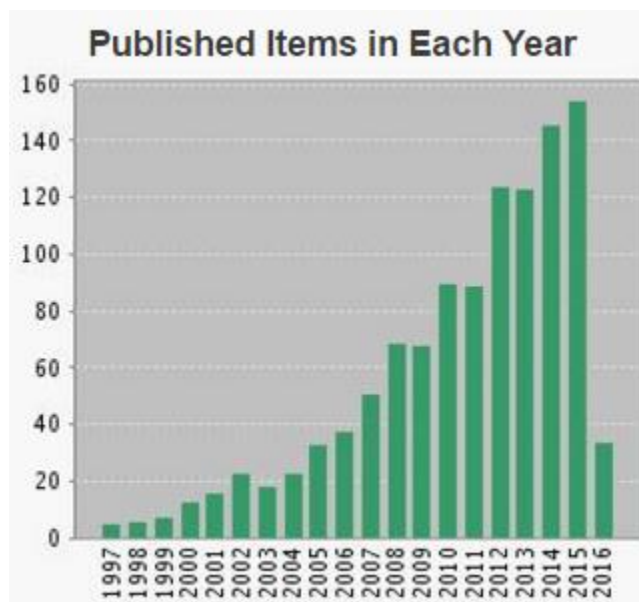
1.2.1. Introduction to Nanoscale Heterogeneous Catalysis

A heterogeneous catalytic reaction involves adsorption of reactants from a solution phase onto a solid surface, surface reaction of the adsorbed species, and desorption of

products into the solution phase.²¹ A heterogeneous material with a smaller particle size will have a higher percentage of its total number of atoms on its surface,²² leading to a higher number of sites for a reactant particle to be adsorbed. This increase in adsorption sites per volume of material leads to the increased catalytic performance of nanoscale materials over microscale materials.²² As the particle size of a heterogeneous material approaches 1-10 nm it starts to take on properties akin to single atoms, further modifying its catalytic behaviour.²²

Research in this area has been increasing rapidly since the early-to-middle 2000s. A *Web of Science* citation report on the query “nanoscale catalysis” shows that initial publications on the topic began in the mid-to-late 1990s and that an upward trend has been taking place since 2004, reaching a maximum in 2015, the last completed year to date (Figure 8). Early research in this area includes the synthesis of organic nanotubes in 1993,²³ catalysis with polymer-supported nanoscale rhodium particles in 1995,²⁴ nanoscale platinum for catalysis of the hydrogenation of chlorobenzene in 1997,²⁵ and bimetallic nanoparticles for use in polymer catalysis in 1998.²⁶ In a highly cited review article titled, “The Impact of Nanoscience on Heterogeneous Catalysis”, Bell summarizes a number of studies which show that the activity and selectivity of catalyst nanoparticles are strongly dependent on their size.²⁷ Bell gives several specific examples including oxide-supported nanoscale vanadium particles catalyzing oxidative dehydrogenation, the removal of sulfur from petroleum products by nanoscale MoS₂ dispersed on alumina, and gold nanoparticles on a titanium support for oxidation of CO to CO₂.

Figure 8. Web of Science number of publications found for query “nanoscale catalysis”, 1997-2016



1.2.2. Heterogeneous Catalysis with Nanoscale Zero Valent Iron

Nanoscale zero-valent iron (nZVI) has been utilized in many catalytic applications. Since 2010 nZVI has been prepared in several different ways and used in several different types of reactions.^{28,29,30} The overwhelming majority of literature examples involving nZVI are for the remediation of ground water and the removal of contaminants such as arsenic(III)³¹, chromium(VI)³², and E. coli bacteria.³³ However, there are also plenty of examples demonstrating the use of nZVI as a synthetic catalyst in organic transformations. In 2012 Raju *et al.* showed that nZVI was able to efficiently and selectively catalyze the reduction of nitroarene compounds to amines. For instance, 1-(4-aminophenyl)ethanone was reduced from 1-(4-nitrophenyl)ethanone in 96 % yield.²⁸ In 2013 Kelsen *et al.* used nZVI to catalyze the hydrogenation of unsaturated carbon-carbon bonds. They were able

to achieve near quantitative conversion to the saturated product using only 2.4 mol% nZVI.³⁰

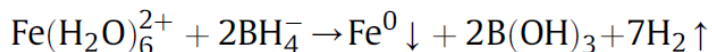
1.2.3. Preparation of Nanoscale Zero Valent Iron

A number of procedures have been shown to synthesize, work up, and store nZVI. By far the most common synthesis is a reduction of an iron(II) or iron(III) salt, such as iron(II) sulfate or iron(III) chloride, to iron(0) by use of sodium borohydride (NaBH₄) in aqueous media. This procedure is inexpensive, uncomplicated and can yield nanoscale iron(0) particles in the range of 10-50 nm.³⁴ The effects of iron and NaBH₄ concentration, atmospheric versus inert conditions, the rate of agitation during reaction, the rate of NaBH₄ addition, and how the iron is dried and stored have been extensively studied and optimized.³⁵ Aging effects on stored nZVI particles have also been studied. In 2014 Zhu *et al.* found that nZVI particles showed no significant differences in size or composition after being exposed to atmospheric conditions in a desiccator for six months.³⁶ It is thought that this is due to the formation of an iron oxide shell which surrounds the amorphous iron(0) upon initial exposure to oxygen. Other publications also reference a core-shell morphology with magnetite (Fe₃O₄) being the main source of iron oxide composing the shell, explaining the particles retaining the black color and magnetic properties also associated with iron(0).^{37,38,39} The use of sodium borohydride as the reducing agent in this synthesis is cheap and easy, but research has shown that there are natural alternatives that avoid the environmental and biological risks associated with its use.⁴⁰

Other methods of preparing nZVI include the decomposition of iron(0) pentacarbonyl⁴¹ and the reduction of goethite [FeO(OH)] by heat and hydrogen gas.⁴² The

requirement of high temperatures and hydrogen gas in these latter two methods make the simpler reduction of an iron(II) or iron(III) salt more appealing for small-scale preparation.

Figure 9. Reduction of an iron salt in aqueous media by sodium borohydride⁵³



1.2.4. Relative Reactivity of Nanoscale Zero Valent Iron

In 2009 Wang *et al.* studied the reactivity of nanoscale iron(0) particles of different sizes and compositions.⁴³ They found that both particle size and the amount of oxidation of the nZVI particles contributed to reactivity - specifically to the ability of the iron to reduce bromate ions in aqueous media. A sample containing iron particles in the range of 5-30 nm outperformed a sample containing particles in the range of 20-50 nm. Opposing this trend were samples of 2-5 nm particles which did not perform as well. This was thought to be due to the additional amount of iron oxides and hydroxides found in this sample as measured by X-ray diffraction analysis.

A year later in 2010 Shih and Tai reacted both nanoscale and microscale zero valent iron (mZVI) with decabrominated diphenyl ether (DBDE) in order to compare the reactivity of each iron species.⁴⁴ Their results showed that nZVI reacted much faster, removing 90% of the DBDE material in only 40 minutes, while the mZVI removed only 40% in the same time frame. In order to achieve 90% removal the mZVI required 40 days and 24-fold more iron. Through their analysis the researchers concluded that nZVI was more reactive than mZVI by a factor of seven.

1.3. An Opiate Model Compound and the Current Work

It is the aim of the current work to take advantage of the enhanced reactivity of nZVI over microscale iron(0) in applying it as the activating agent in a nonclassical Polonovski reaction for the efficient *N*-demethylation of tertiary *N*-methylamines. As described in section 1.1.3, Kok *et al.* showed that commercially available iron(0) powder was a suitable activating agent, but that stoichiometric amounts of iron and chlorinated solvents were necessary in order to provide the best results. It is hypothesized that by decreasing the particle size and thus increasing the total surface area of the iron(0) activating agent, better results in the way of reaction times and amounts of iron required can be achieved. In order to test this hypothesis, the pseudo opiate dextromethorphan was chosen as an ideal substrate for a number of reasons: it is structurally similar to naturally occurring opiates; unlike naturally occurring opiates it is not a highly controlled substance and so is comparatively easy and inexpensive to obtain commercially; the hydrobromide and hydrochloride salts are atmospherically stable solids at room temperature making them easy to work with; it is easily transformed into the *N*-oxide derivative in high yields; and perhaps most importantly, it was one of the compounds analyzed in the previously mentioned 2010 study which provides a direct comparison with the current work.

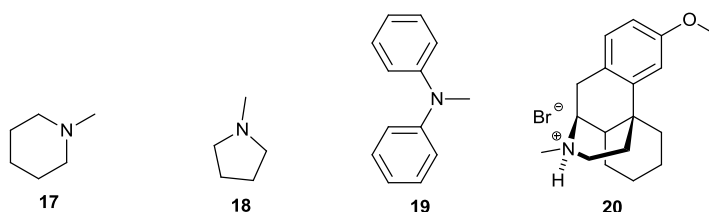
2. Results and Discussion

2.1. Preparation and Characterization of Substrates

The scope of the *N*-demethylation of tertiary amines was of primary interest. Hence, the choice of substrates to be initially used was among the first things considered for this work. Because naturally occurring opiate compounds are under strict government

regulation the choice of model compounds was restricted to commercially available *N*-methyl tertiary amines. The first choice of model compound was the pseudo-opiate dextromethorphan (DXM) sold commercially as its hydrobromide salt **20**. This compound would serve as an ideal substrate given its structural similarity to natural opiates and its use in previous studies of the Polonovski reaction.²⁰ However, there are some controls on DXM resulting in delays in its delivery. Other commercially available and more accessible compounds considered were *N*-methylpiperidine, **17**, *N*-methylpyrrolidine, **18**, and *N*-methyldiphenylamine **19**, shown in Figure 10.

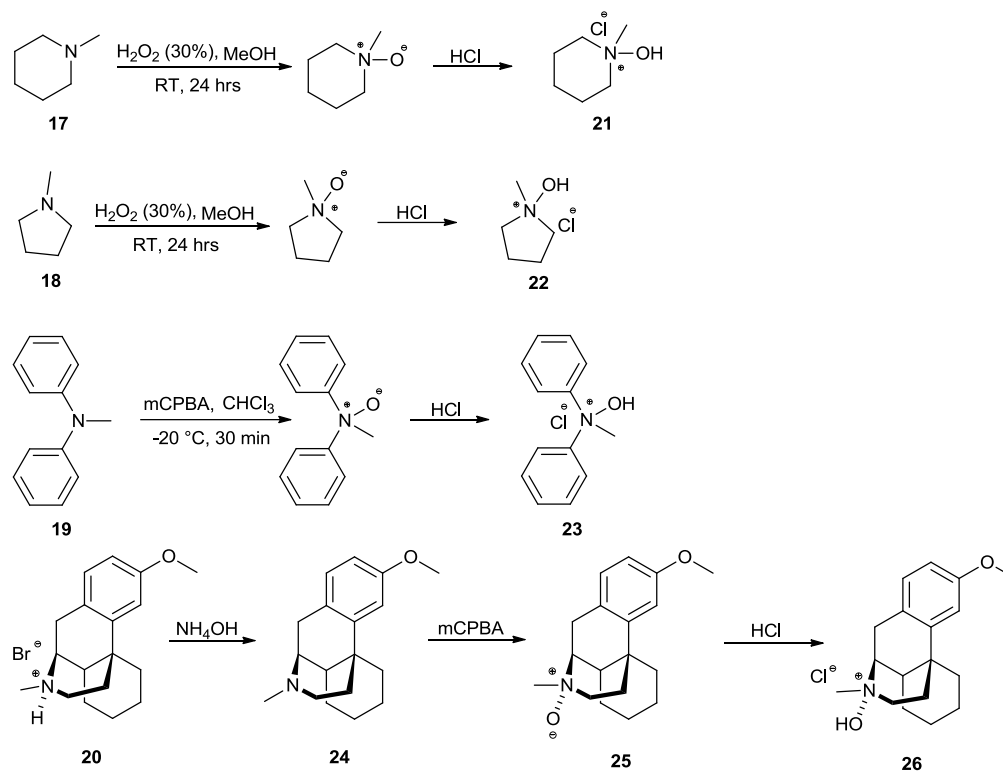
Figure 10. Structures of tertiary methylamine substrates



The first two of these compounds, **17** and **18** were available in our laboratory from previous work while the third, *N*-methyldiphenylamine **19**, would need to be purchased or synthesized. Due to the availability of diphenylamine in the lab an attempt was made to synthesize the compound by reacting the diphenylamine with methyl iodide in dry acetone according to the literature.⁴⁵ However, even after 98 hours at reflux temperature it was found by GC-FID that only 1/3 of the diphenylamine had been converted to product. Such low yields were surprising and it was speculated that reagents or solvents were not completely anhydrous or that the volatile methyl iodide was escaping the reaction flask during reflux. Whatever the reason for the failed reaction it was decided that in the interest of time **20** would be purchased instead of being synthesized.

With the three substrates procured, the next step was converting each to its *N*-oxide hydrochloride derivative, as shown in Figure 11. In the case of **17** and **18**, which are water

Figure 11. Proposed synthesis of substrate *N*-oxide compounds



soluble, a 30 % (w/w) aqueous solution of hydrogen peroxide was added to a methanol solution of the substrate and stirred for 24 hours at room temperature. Magnesium oxide was used to destroy any remaining peroxide species and the reaction mixture was acidified with 6 M HCl and concentrated to dryness. The resulting materials were washed with dimethyl ether to afford *N*-methylpiperidine *N*-oxide hydrochloride, **21**, and *N*-methylpyrrolidine *N*-oxide hydrochloride, **22**. The isolated yield of **21** was 88 % while **23** was 78%. The ^1H -NMR peak assignments of **21** and **22** are shown in Figures 12 and 13 respectively.

Figure 12. $^1\text{H-NMR}$ spectra of *N*-methylpiperidine *N*-oxide hydrochloride, **21**, with peak assignments

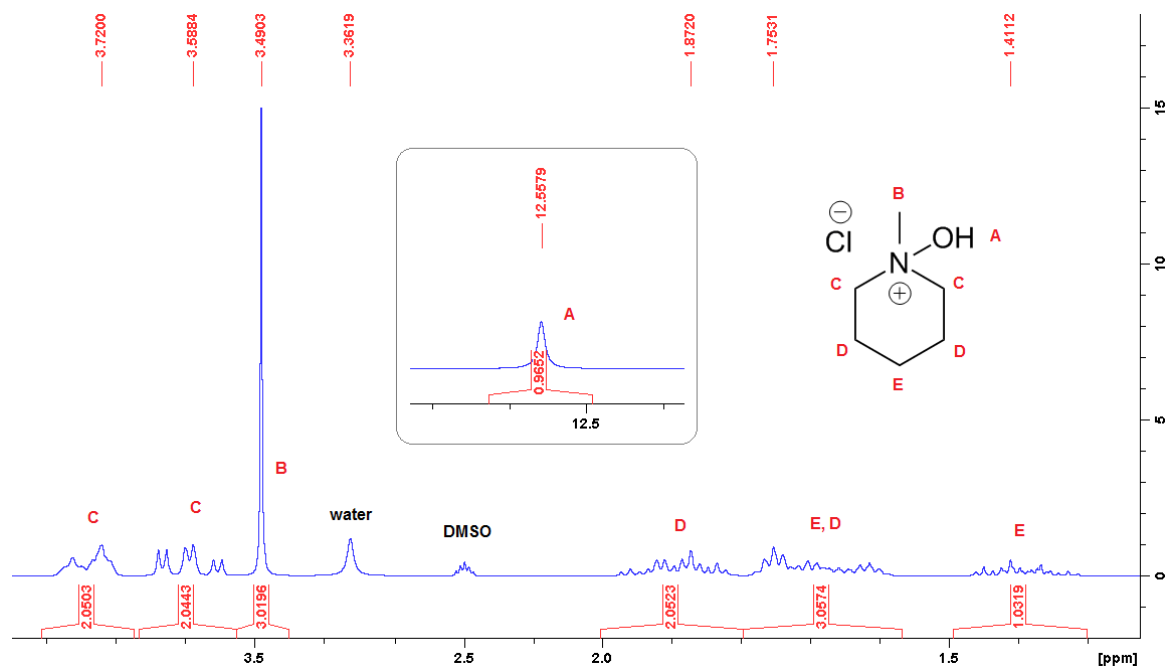
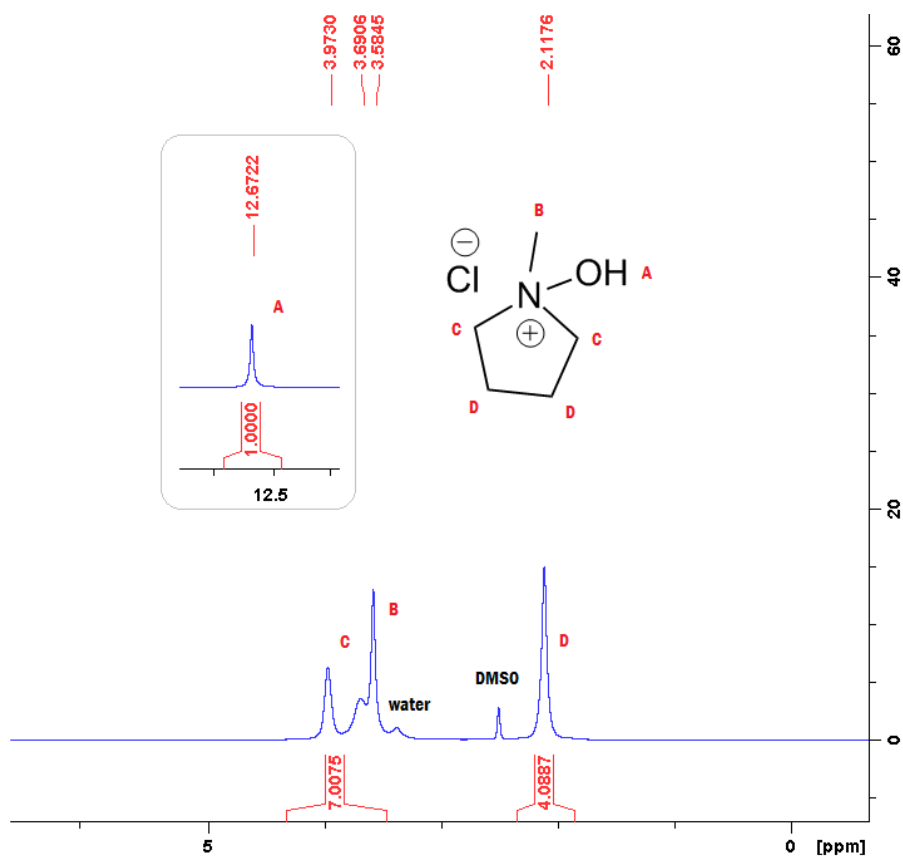


Figure 13. $^1\text{H-NMR}$ spectra of N-methylpyrrolidine N-oxide hydrochloride, **22**, with peak assignments



Elemental analysis (EA) and mass spectroscopy (ESI-MS) were also used to characterize these species and the details are given in Section 5. The integration and chemical shift values of the $^1\text{H-NMR}$ spectra of **21** and **22** show the expected 14 and 12 protons respectively with the expected chemical shifts. Elemental analysis confirms that **21** is 48 % carbon, 9 % hydrogen and 9 % nitrogen and that **22** is 43 % carbon, 9 % hydrogen and 10 % nitrogen. One point of interest came from the mass spectra of these compounds. The spectrum of **21** shows the $[\text{M}]^+$ peak as the dimer at 231.2 m/z instead of the expected 116.1 m/z, which was present as a smaller peak (31 % intensity of $[\text{M}]^+$ peak). This was the result of one proton being eliminated from one molecule of **21** in the

electrospray nebulizer, or elsewhere in the MS process, that then formed a dimer with another molecule of **21** prior to being detected by the ion trap. MS/MS of the peak at 204.1 m/z supports this analysis. The $[M]^+$ peak of **22** is present at 103.2 m/z and there is also a peak at 204.1 m/z (58 % intensity) which appears to represent the dimer as in the spectrum of **21**.

The synthesis of **23** proved to be challenging and a pure sample was not obtained. Hydrogen peroxide could not be used as the oxidizing agent due to the limited water solubility of **19**. Alternatively, the organic soluble metachloroperoxybenzoic acid (mCPBA) in chloroform was used instead and the reaction mixture was stirred at room temperature for 3 hours. Excess mCPBA and by-products were removed *via* basic aqueous extraction and the organic layer was concentrated to dryness presenting what appeared to be at least two product species of various shades of a deep blue color, one of which was a low-viscosity oil and the other a powder. $^1\text{H-NMR}$ did not show any evidence of the OH proton of the *N*-oxide group for **23**. Hence, it was evident that the synthesis of this compound did not proceed as expected and the compound was not used in any later work.

While initial *N*-demethylation reactions were performed on **21**, it was soon realized that isolating the demethylated product from any by-products and solvent would be more time consuming and technically challenging than anticipated due to the high volatility of both the starting materials and, even more so, the products. After some consideration it was decided that because DXM offered several advantages as an opiate model compound over the three small molecules **17**, **18** and **19** (being closer in structure to naturally occurring opiates, having comparatively low volatility, and having been previously studied as a

substrate in the Polonovski reaction), efforts would be shifted away from these small molecules and toward DXM as the potential lone substrate of interest.

As with the previous substrates, the purchased DXM-HBr, **20**, first had to be converted to, and isolated as, the *N*-oxide hydrochloride derivative. To achieve this, **20** was dissolved in chloroform followed by deprotonation that was performed in a separatory funnel using concentrated ammonium hydroxide. The organic layer was then cooled to -20 °C and stirred with 1.5 equivalents of mCPBA to afford the *N*-oxide, **25**. Acidification with HCl produced the *N*-oxide hydrochloride, **26**, in 84 % yield. **26** was characterized by IR, ¹H-NMR, ¹³C-NMR, ¹H-NMR COSY, ESI-MS and EA. Peaks of the ¹H-NMR spectrum (Figure 14) were assigned by the use of the COSY spectrum (Figure 15) and NMR prediction software.

Figure 14. $^1\text{H-NMR}$ COSY spectra of DXM *N*-oxide hydrochloride

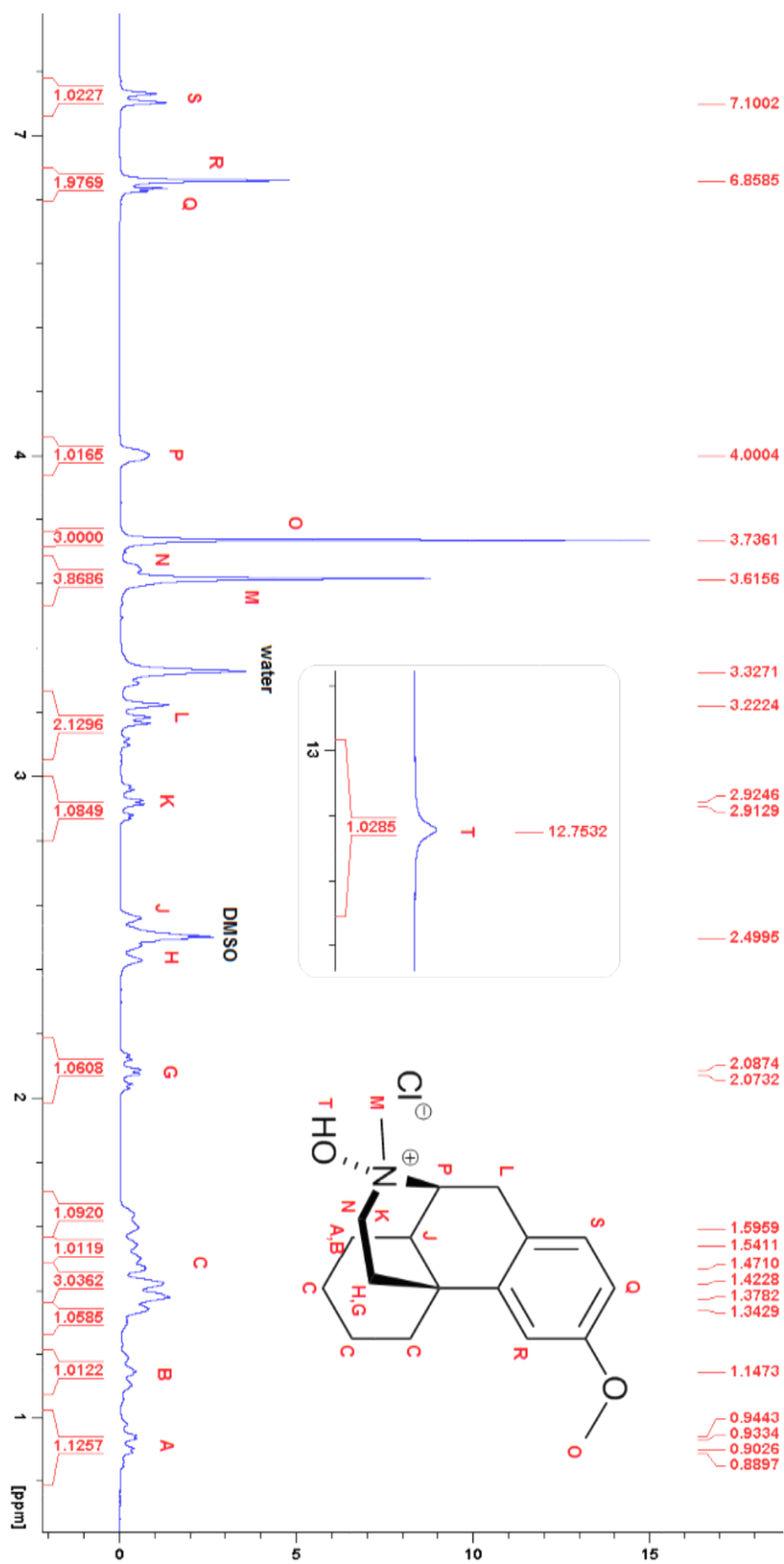
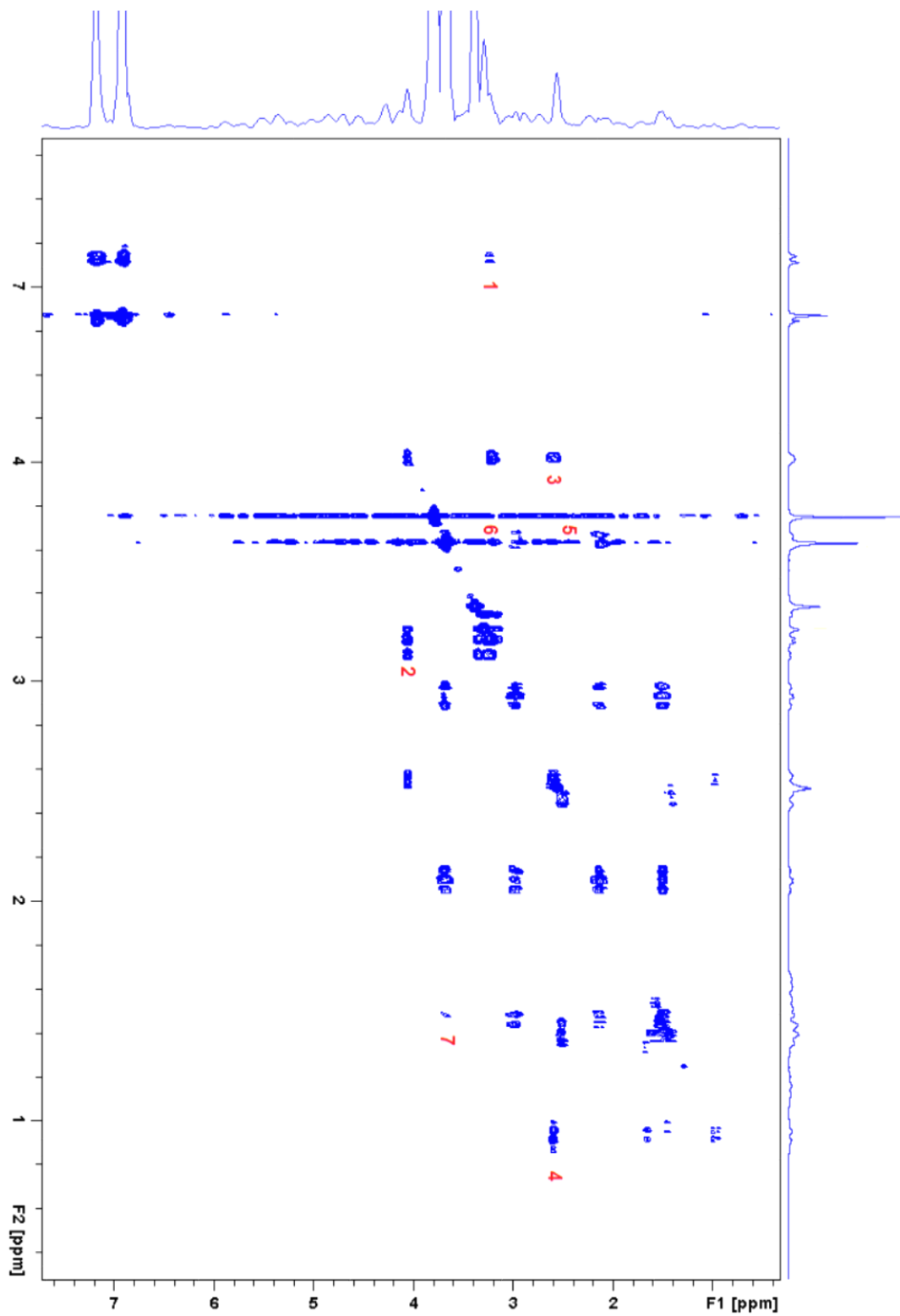


Figure 15. $^1\text{H-NMR}$ COSY spectra of DXM *N*-oxide hydrochloride, with peak assignments



In the following description of the peak assignments, peaks referred to by letter (A-P) are located on the 1D ^1H -NMR spectrum (Figure 14) whereas peaks referred to by number (1-7) are located on the 2D COSY spectrum (Figure 15). Peak 1 shows a correlation between an aromatic proton and the protons at 3.22 ppm, leading to the assignment of the protons marked L. These two L protons correlate to the proton marked P (peak 2), and in turn, peak 3 shows a correlation between proton P and J, enabling their assignments. Peak 4 shows proton J correlating to peaks A and B, giving their assignment. The only remaining position directly adjacent to the nitrogen atom is assigned to the peak at 3.62 ppm, N. The COSY spectrum shows peaks marking correlations between N and G (peak 5) and N and K (peak 6). Peak 6 appears to be a larger peak and so the proton marked G is assigned as being one carbon away from N, and K is assigned as the proton on the same carbon as N. At this point the only protons which remain unassigned are the aliphatic protons marked C and the proton marked H. H is assigned based on its apparent correlation with N (peak 7), and the remainder are left as a multiplet with integration of 5 due to a lack of resolution in both spectra. Finally, the hydroxylic proton of the *N*-oxide group is not present due to hydrogen/deuterium exchange.

2.2. Preparation and Characterization of Nanoscale Zero Valent Iron

The next step was to synthesize nanoscale zero valent iron (nZVI) which would be utilized as the activating agent in the modified Polonovski *N*-demethylation reaction of DXM. Following the procedure of Moores *et al.*³⁴, iron(II) sulfate heptahydrate was reduced in aqueous media by sodium borohydride with mechanical stirring, washed with water and then methanol *via* repetitions of centrifugation, decantation, and replacement of solvent, and finally suspended in the reaction solvent. This suspension was then added to

the reaction flask containing the *N*-oxide species dissolved in the same solvent. Characterization of the nZVI was done on the TESCAN MIRA 3 LMU Variable Pressure Schottky Field Emission Scanning Electron Microscope at Saint Mary's University. Figures 16 and 17 are images of the synthesized nZVI taken by the SEM (Figure 16).

Figure 16. SEM image of lab-synthesized nZVI, 500 nm scale

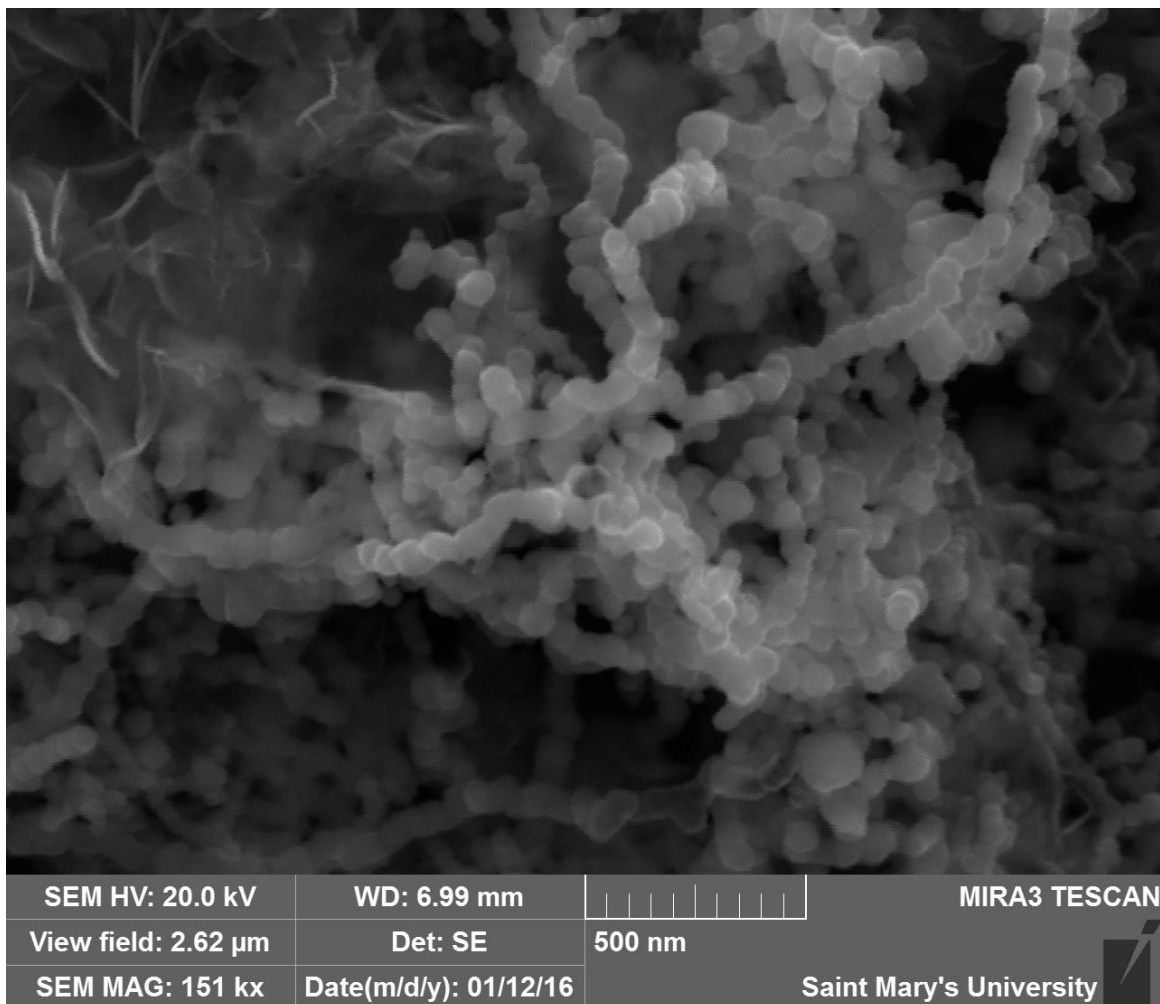
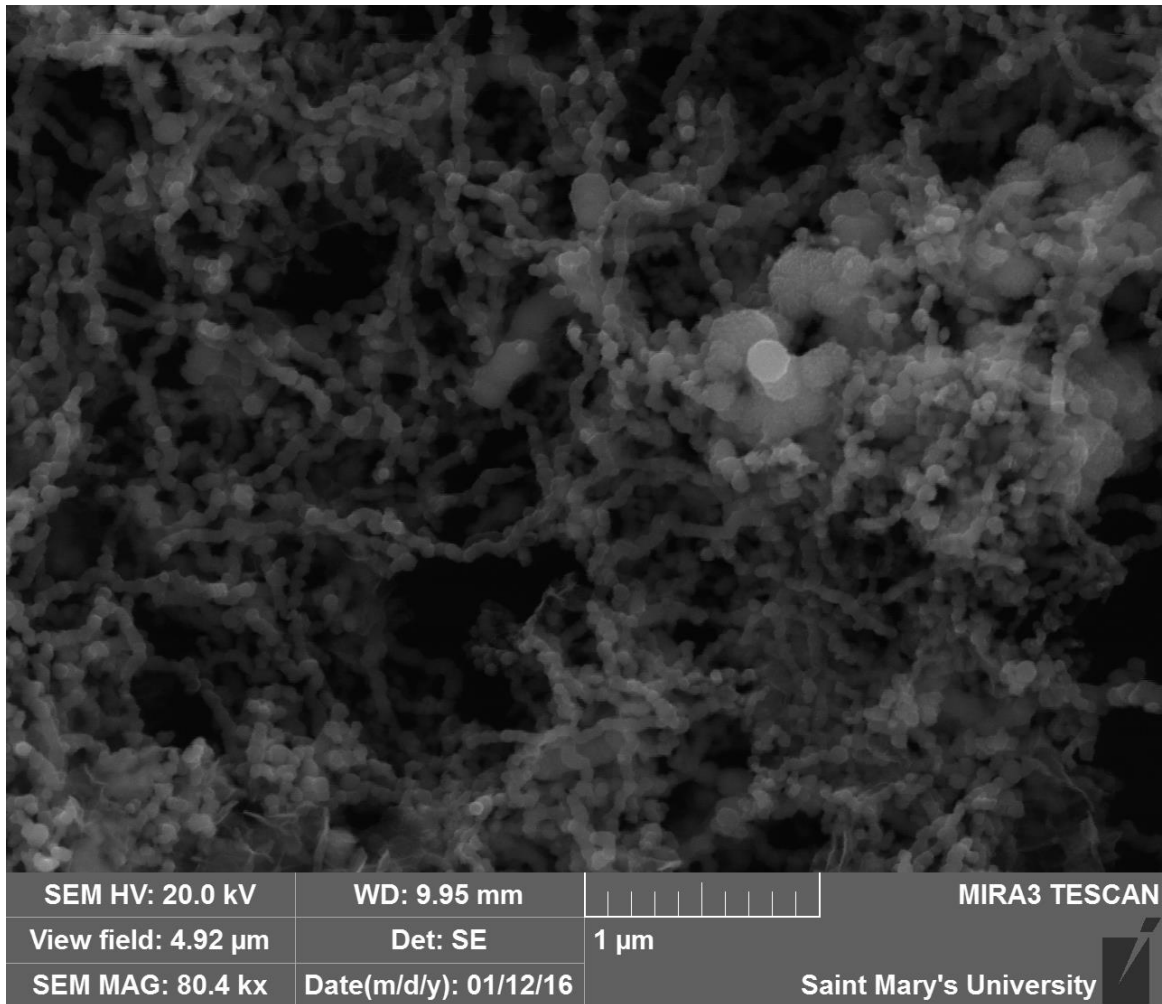
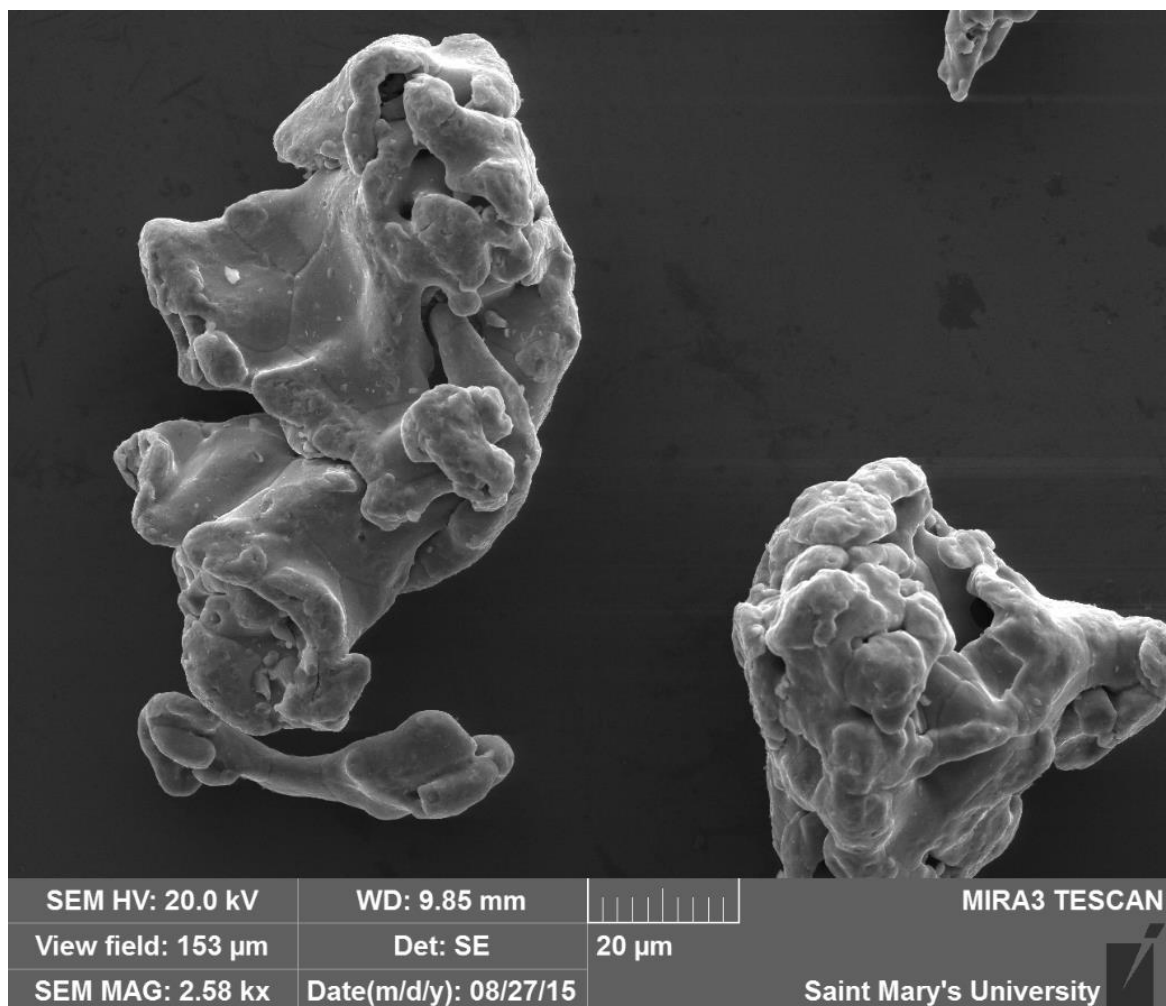


Figure 17. SEM image of lab-synthesized nZVI, 1 μm scale



nZVI particles range in size from approximately 50 to 200 nm with the majority under 100 nm. Significant agglomeration of particles had taken place between the time of their formation and when they were observed using SEM, which was approximately one hour. Evidence of this aggregating behaviour of nZVI has been widely reported in the literature.^{34,35,46} Iron(0) dust, used by Kok *et al.* in their 2010 study, was also characterized by SEM (Figure 18). Images show amorphous particles approximately 50 μm in size.

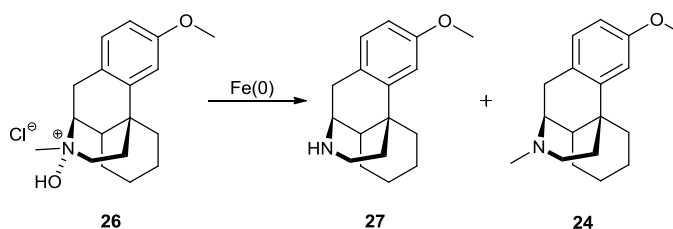
Figure 18. SEM image of a commercially available iron(0) dust



2.3. *N*-demethylation Reactions

Before continuing to the demethylation step it is important to note that Kok *et al.* showed that the results obtained from an iron-mediated nonclassical Polonovski reaction depended heavily on the reaction solvent chosen. Whereas 97 % yield of the demethylated product **27** (Figure 19) was obtained after 1 hour in chloroform, only 59 % was obtained after 3 hours in methanol and 89 % after 21 hours in isopropanol. This disparity inspired

Figure 19. Proposed synthetic pathway of *N*-nordextromethorphan, **27**



the current work to also investigate multiple solvents in order to gain a more complete picture of the comparative reactivity of nZVI as a modified Polonovski activating agent. It was initially thought that additional reactivity of nZVI may lower the reaction time in isopropanol from 21 hours to something approaching the 1 hour observed when chloroform was used. Furthermore, an alcoholic solvent in place of a chlorinated one would represent a much more environmentally friendly, green synthesis. For these reasons, isopropanol was the first solvent examined. An initial experiment was conducted to verify the results found by Kok *et al.* Hence, DXM *N*-oxide hydrochloride, **26**, was reacted with one equivalent of commercially available iron(0) dust (from here on referred to as “iron(0) dust”). Alternatively, one equivalent of the freshly synthesized nanoscale zero valent iron (nZVI) was used in a parallel experiment. It was found that the iron(0) dust reaction yielded 84.2 % *N*-norDXM, **27**, while the nZVI yielded 86.8 %. These were comparable to the previous results indicating that the reactions were proceeding as expected. In order to compare the performance of the two iron sources in isopropanol a set of parallel reactions were conducted for 16 hours. By reducing the reaction time it was theorized that the additional reactivity of nZVI should produce a higher yield of the desired product than the iron(0) dust. The results of these reactions, run in triplicate, are summarized in Table 2.

Table 2. Results of *N*-demethylation of DXM in isopropanol at room temperature with reduced reaction time

Entry	Trial	Activating Agent	Reaction Time (hrs)	Solvent	Isolated Yield <i>N</i> -norDXM (mol %)
1	1	Fe(0) dust, 1 eq.	16	<i>i</i> -PrOH	79.8
2	2	Fe(0) dust, 1 eq.	16	<i>i</i> -PrOH	82.5
3	3	Fe(0) dust, 1 eq.	16	<i>i</i> -PrOH	83.0
4	1	nZVI, 1 eq.	16	<i>i</i> -PrOH	84.9
5	2	nZVI, 1 eq.	16	<i>i</i> -PrOH	81.7
6	3	nZVI, 1 eq.	16	<i>i</i> -PrOH	86.1

The average isolated yield of these trials was 81.7 ± 1.71 and 84.2 ± 2.27 for the iron(0) dust and nZVI respectively. A T-test at the 95 % confidence interval reveals that there is not a significant enough difference between the two mean values to say that they are statistically different. In other words, the nZVI did not conclusively outperformed the iron(0) dust in these reactions.

Following the same framework used for the reactions in isopropanol, chloroform was the next solvent to be examined. Kok *et al.* showed that a maximum yield of 97 % *N*-norDXM was achieved in one hour in chloroform using iron(0) dust. Attempting to reproduce that result, one hour reactions were performed in chloroform using both sources of iron. Iron(0) dust produced a 95 % yield while nZVI produced 92 %. As with the reactions conducted in isopropanol the reaction time was reduced to show any potential

difference in performance between iron(0) dust and nZVI. These reactions were run only once instead of in triplicate and are summarized in Table 3.

Table 3. Results of *N*-demethylation of DXM in chloroform at room temperature with reduced reaction time

Entry	Activating Agent	Reaction Time (hrs)	Solvent	Isolated Yield <i>N</i>-norDXM (mol %)
1	Fe(0) dust, 1 eq.	0.5	CHCl ₃	69.2
2	nZVI, 1 eq.	0.5	CHCl ₃	75.4

In these experiments a difference of 6.2 % in isolated yield when nZVI is used compared to iron(0) dust was observed. While this difference is larger than what was seen in isopropanol, it is still possible that it does not represent a real increase due to the previously shown variance between measurements. To determine a statistical difference in the two methods at least three trials of each experiment should be conducted and compared.

The third and final solvent to be examined was methanol. Once again looking to the literature, Kok *et al.* showed that an optimal reaction time when using iron(0) dust in methanol was three hours and that such reactions generated a 59 % isolated yield of *N*-norDXM. Equivalent reactions in our lab produced 74 % and 59 % for iron(0) dust and nZVI respectively. Reaction times were again reduced to produce the results seen in Table 4.

Table 4. Results of *N*-demethylation of DXM in methanol at room temperature with reduced reaction time

Entry	Activating Agent	Reaction Time (hrs)	Solvent	Isolated Yield <i>N</i> -norDXM (mol %)
1	Fe(0) dust, 1 eq.	0.5	MeOH	65.4
2	nZVI, 1 eq.	0.5	MeOH	52.2

In these reactions the iron(0) dust out-performs the nZVI. The iron(0) dust also out-performs what was found by Kok *et al.* in 2010. As mentioned above, when this reaction is carried out for three hours a similar trend was noted; the iron(0) dust out-performs what has been reported in the literature whereas the nZVI produces yields more in agreement with what is reported in the literature. These results were surprising and are not understood.

The second hypothesis in need of investigation was that the added reactivity of nZVI could produce superior results to iron(0) dust at lower than stoichiometric levels of loading. According to the reaction scheme proposed by McCamley *et al.* in Figure 7, iron may be viewed as a catalytic species in the modified Polonovski reaction. Reactions therefore were carried out with only 10 mol % amounts of iron at the optimal reaction times found by Kok *et al.* In Table 5, all three reaction solvents were included in this set of experiments.

Table 5. Results of *N*-demethylation of DXM in various solvents using less than a stoichiometric amount of activating species

Entry	Activating Agent	Reaction Time (hrs)	Solvent	Isolated Yield <i>N</i>-norDXM (mol %)
1	Fe(0) dust, 0.1 eq.	21	<i>i</i> -PrOH	58.5
2	Fe(0) dust, 0.1 eq.	1	CHCl ₃	70.4
3	Fe(0) dust, 0.1 eq.	3	MeOH	64.1
4	nZVI, 0.1 eq.	21	<i>i</i> -PrOH	78.0
5	nZVI, 0.1 eq.	1	CHCl ₃	66.6
6	nZVI, 0.1 eq.	3	MeOH	34.0

Once again the iron(0) dust outperformed the nZVI in methanol. While the nZVI produced similar results to iron(0) dust in chloroform, it did fare quite a lot better in isopropanol. In isopropanol a 19.5 % increase in the isolated yield is observed when nZVI is used. Following the observation of this performance increase in isopropanol at 10 mol % loading, it was thought worthwhile to look back at Table 2 which shows the results of the initial isopropanol experiments. It is possible that within the 16 hour reaction time the nZVI experiments reached a maximal yield, causing the performance gap between iron(0) dust and nZVI to be understated. Supporting this hypothesis is the fact that the 16 hour nZVI reactions achieved an average yield (84.2 %) very similar to the 21 hour reaction (86.8 %). In other words, it could be that the reaction time was long enough to allow the iron(0) dust reaction to “catch up” to the nZVI reaction, which had reached a maximal yield some time before. In order to examine this, reactions with iron(0) and nZVI in isopropanol

were run for a shorter period of time, such that the yield should be significantly below optimal. These results are given in Table 6.

Table 6. Results of *N*-demethylation of DXM in isopropanol at room temperature with further reduced reaction time

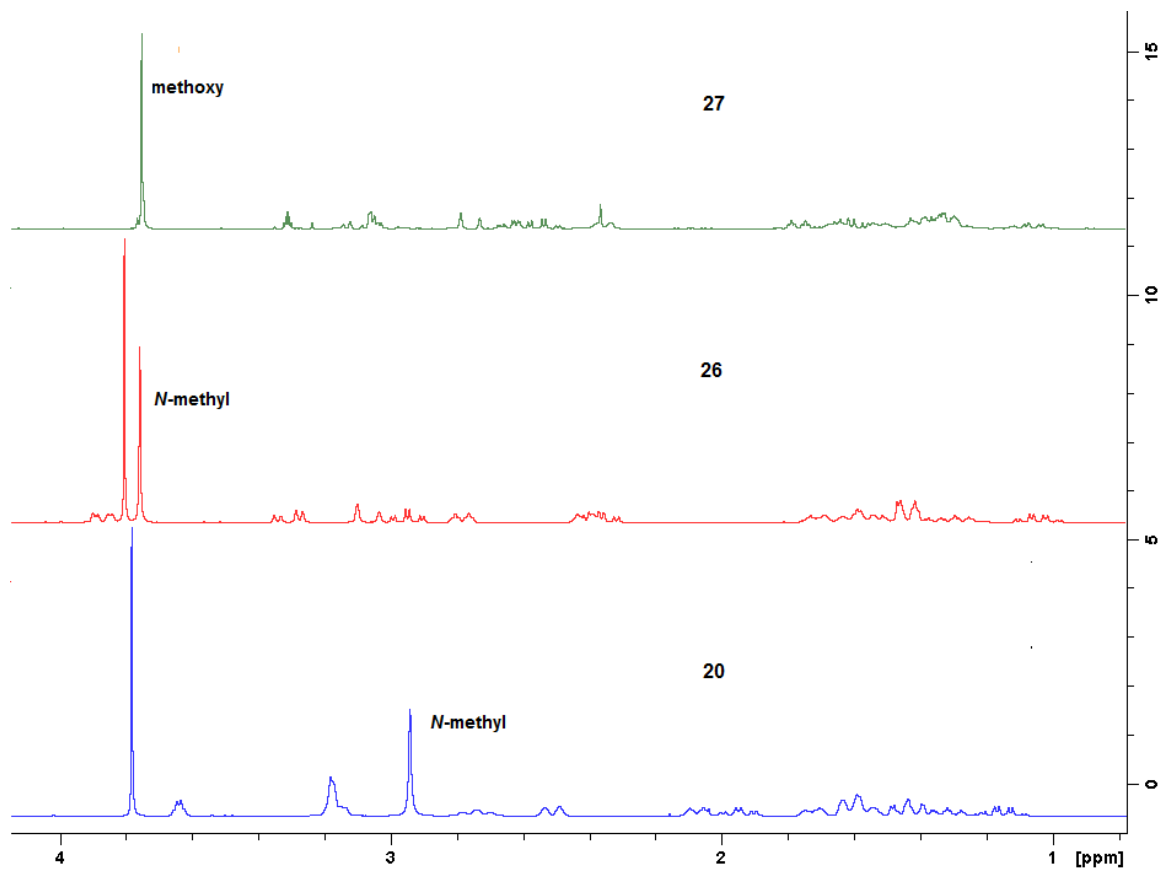
Entry	Activating Agent	Reaction Time (hrs)	Solvent	Isolated Yield <i>N</i> -norDXM (mol %)
1	Fe(0) dust, 1 eq.	7	<i>i</i> -PrOH	62.9
2	nZVI, 1 eq.	7	<i>i</i> -PrOH	83.6

When the reaction time was reduced to approximately 1/3 the time required for a complete reaction a significant difference between the iron(0) dust and nZVI was observed. When iron(0) dust was used the isolated yield of **27** was 62.9 %, whereas nZVI yielded 83.6 %. This result supports the argument that previous 16 hour reactions in isopropanol were allowing both sources of iron to achieve a maximum yield and shows that nZVI has increased the rate of this reaction. Also of note is that an 83.6 % yield was similar to the yields produced by both iron(0) dust and nZVI when reactions times were 16 and 21 hours, suggesting that this seven hour reaction may have also reached a maximum yield.

Characterization of *N*-norDXM and DXM isolated from these reactions were done by ¹H-NMR, ¹³C-NMR, and mass spectroscopy. The ¹H-NMR spectra of **20**, **26**, and **27** are shown in Figure 20 and agree with those reported in the literature.^{47,48} The most identifiable differences and similarities between the spectra are seen in the peaks representing the methyl groups. Each of the three spectra contain the same methoxy protons, the peak of which is located around 3.8 ppm on each spectra. The other methyl group is the *N*-methyl

group and the peak representing these protons is present only in species **20** and **26** (at approximately 2.95 ppm in **20** and 3.75 ppm in **26**). This peak's disappearance in the spectra of **27** is evidence that the *N*-demethylation reaction was successful.

Figure 20. Comparison between ^1H -NMR spectra of DXM-HBr, **20**, DXM *N*-oxide HCl, **26**, and *N*-norDXM, **27** (aromatic regions removed for size)



3. Conclusion

N-oxide hydrochloride derivatives of *N*-methylpiperidine, **18**, *N*-methylpyrrolidine, **19** and dextromethorphan, **24**, were successfully synthesized and characterized by ¹H-NMR, ¹³C-NMR, IR, ESI-MS, and EA. Nanoscale zero valent iron was synthesized by the reduction of iron(II) sulfate heptahydrate and characterized by SEM. nZVI has been shown to be an effective activating agent for the *N*-demethylation of dextromethorphan in a variety of solvents. It was found that in isopropanol a stoichiometric amount of nZVI was able to achieve an 83.6 % yield of the demethylated product, **27**, compared to 62.9 % for a stoichiometric amount of a previously studied iron(0) dust. This result confirms the hypothesis that using smaller iron particles as the source of activating agent causes the nonclassical, modified Polonovski reaction originally studied by Kok *et al.* to proceed at a higher rate.

Additionally, 10 mol % nZVI in isopropanol for 21 hours yielded a 78.0 % isolated yield of **27** whereas 10 mol % iron(0) dust achieved only 58.5 %. This indicates the same rate increase as previously stated as well as confirms that iron is catalytic in this reaction.

Finally, solvents played an important role in these reactions; performance gained by using nZVI in isopropanol was not replicated in reactions performed in methanol or chloroform.

4. Future Directions

Further testing of the reactivity of nZVI as the activating agent in a nonclassical, modified Polonovski reaction should be undertaken in order to determine the optimal reaction times and iron loading in a variety of solvents. Each reaction which was performed only

once in the current work should be performed in triplicate to provide additional confidence in its result. Additionally, an ionic liquid solvent should be tested.

From the SEM images of nZVI in Figures 16 and 17, it is clear that the synthesized nanoparticles have significantly agglomerated. This agglomeration reduces the surface area and number of available reaction sites of the iron particles. A comparative study of some of the many different methods of increasing colloidal stability which are found in the literature would be of great value. Shi, Zhang, and Chen found that the ability of nZVI to remove chromium(IV) ions from waste water was increased by the addition of bentonite (an absorbent aluminium phyllosilicate clay) as a support material.⁴⁹ When nZVI is prepared by sodium borohydride reduction of an iron(II) or iron(III) salt, the bentonite is simply added to the reaction flask during reduction. Many different polymer materials have also been used to increase the colloidal stability of nZVI. Moores *et al.* investigated four such polymers and found that each significantly increased the colloidal stability of nZVI when added before or after the reduction of an iron(II) or iron(III) salt.³⁴

Plotting the concentration of demethylated product versus time and determination of a pseudo first order rate constant would provide insight into the kinetics of these reactions and might help to optimize reaction conditions. These experiments would be relatively simple to perform as a slightly modified version of the current methodology could be used.

5. Experimental

5.1. General Methods

Iron(0) dust, iron(II) sulfate heptahydrate, and dextromethorphan hydrobromide were purchased from Sigma Aldrich and stored under atmospheric conditions. Sodium borohydride was purchased from Caledon Laboratory Chemicals in 2010 and stored under atmospheric conditions. All other reagents and solvents were purchased from various chemical suppliers and used as received.

Nuclear Magnetic Resonance spectra were obtained from a Bruker 300 MHz Ultrashield spectrometer. All ^1H and ^{13}C experiments were conducted at 300 and 75 MHz respectively. Chemical shifts (δ ppm) were referenced with solvent residual peaks. Deuterated NMR solvents DMSO- d_6 and chloroform- d were purchased from Cambridge Isotope Laboratories. Methanol- d_4 was purchased from Sigma Aldrich.

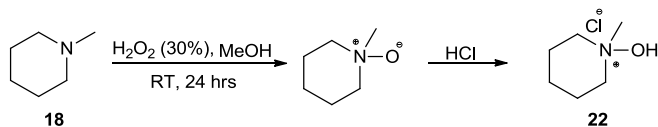
A Caframo Compact Digital BDC 2002 mechanical stirrer and a Clay Adams Compact II centrifuge were used in the synthesis of nZVI. An Electrothermal Mel-Temp 3.0 melting point apparatus was used to obtain melting point data. Electrospray ionization mass spectrometry and elemental analysis (CHN) samples were prepared in our research lab and sent to Patricia Granados at the Saint Mary's University Center for Environmental Analysis and Remediation (CEAR) for processing using an Agilent 1100 LC/MSD Trap and Perkin Elmer 2400 Series II CHN Analyzer respectively. IR spectra were obtained from a Bruker ALPHA Infrared Spectrometer by use of the attenuated total reflection (ATR) sampling technique.

All *N*-oxide synthesis and *N*-demethylation reactions were carried out under atmospheric conditions. All *N*-demethylation reactions were conducted at room temperature.

5.2. Synthesis of *N*-oxide Hydrochloride salts

5.2.1. Synthesis of *N*-methylpiperidine *N*-oxide Hydrochloride

Figure 21. Synthesis of *N*-methylpiperidine *N*-oxide hydrochloride

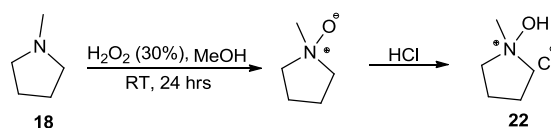


Following a modified procedure,⁵⁰ 4.1 g (41.1 mmol) of *N*-methylpiperidine, **17**, in 50 mL of methanol was cooled to near 0 °C in an ice bath and to it was added 15 molar equivalents of a 30 % (w/w) aqueous solution of hydrogen peroxide. The mixture was stirred at room temperature for 24 hours. The reaction mixture was again cooled to near 0 °C and magnesium oxide was added in small portions to destroy any residual peroxides until KI / starch paper showed no remaining presence of peroxides. The reaction mixture was then filtered through a Celite pad and the pad was washed with methanol. The filtrate and washings were combined, concentrated to dryness, dissolved in chloroform and extracted with 6 M HCl (pH 2). The organic layer was concentrated to dryness to afford the *N*-oxide hydrochloride derivative, **21**, as a white powder which decomposes at temperatures above 115 °C (36.5 mmol, 89 %). IR (ATR): 2730.7 (s), 2652.8 (vs, OH stretch), 2570.1 (s), 2515.8 (s), 1544.3 (s), 1439.5 (s), 744.0 (vs, OH bend). ¹H NMR (DMSO-*d*₆, 300 MHz) δ 12.56 (s, 1H), 3.72 (m, 2H), 3.59 (m, 2H), 3.49 (s, 3H), 3.36 (s, 1H), 1.98-1.80 (m, 2H), 1.80-1.57 (m, 3H), 1.49-1.30 (m, 1H). ¹³C NMR (DMSO-*d*₆, 75

MHz) δ 64.57, 56.64, 20.53. ESI-MS (+): Calcd for C₆H₁₄NO m/z: 116.18. Found m/z: 231.1, 116.1. Anal. Calcd for [C₆H₁₄NO]⁺Cl⁻: C, 47.53; H, 9.31; N, 9.24. Found: C, 47.55; H, 8.87; N, 9.24.

5.2.2. Synthesis of *N*-methylpyrrolidine *N*-oxide Hydrochloride

Figure 22. Synthesis of *N*-methylpyrrolidine *N*-oxide hydrochloride

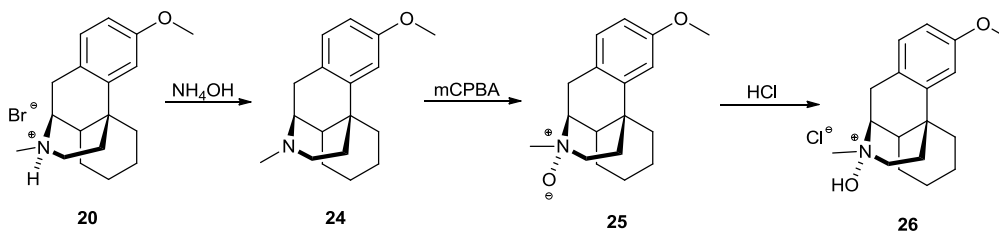


Following a modified procedure,⁵⁰ 2.0 g (23.5) mmol of *N*-methylpyrrolidine, **18**, in 20 mL of methanol was cooled to near 0 °C in an ice bath and to it was added 15 molar equivalents of a 30 % (w/w) aqueous solution of hydrogen peroxide. The mixture was stirred at room temperature for 24 hours. The reaction mixture was again cooled to near 0 °C and magnesium oxide was added in small portions to destroy any residual peroxides until KI / starch paper showed no remaining presence of peroxides. The reaction mixture was then filtered through a Celite pad and the pad was washed with methanol. The filtrate and washings were combined, concentrated to dryness, dissolved in chloroform and extracted with 6 M HCl (pH 2). The organic layer was concentrated to dryness to afford the *N*-oxide hydrochloride salt **22** as a light brown powder which decomposes at temperatures above 115 °C (17.3 mmol, 74 %). IR (ATR): 2711.3 (m), 2611.7 (vs, OH stretch), 2454.2 (m), 1536.0 (s), 1448.0 (s), 757.5 (vs, OH bend). ¹H NMR (DMSO-d₆, 300 MHz) δ 12.65 (1H), 3.95 (2H), 3.69 (4H), 3.59 (3H), 2.12 (4H). ¹³C NMR (CDCl₃, 75 MHz) δ 68.08, 53.83, 21.96. ESI-MS (+): Calcd for C₅H₁₂NO m/z: 102.09. Found m/z:

103.2, 204.1. Anal. Calcd for $[C_5H_{12}NO]^+Cl^-$: C, 43.64; H, 8.79; N, 10.18. Found: C, 43.23; H, 8.95; N, 10.05.

5.2.3. Synthesis of Dextromethorphan *N*-oxide Hydrochloride

Figure 23. Synthesis of dextromethorphan *N*-oxide hydrochloride



Following the procedure outlined by McCamley *et al.*¹⁹, 3.0 g (8.1 mmol) of DXM-HBr, **20**, in 60 mL chloroform was extracted with concentrated ammonium hydroxide (pH 10) and the organic layer, containing dextromethorphan, **24**, was cooled to -20 °C in a dry ice/acetone bath. To the solution was added 1.1 molar equivalents of mCPBA all in one portion. The mixture was stirred for 30 minutes at -20 °C and gravity filtered to afford DXM *N*-oxide **25** in solution. The filter pad was washed with chloroform and the filtrate and washings were combined and loaded into a separatory funnel. The solution was then extracted twice with NaOH/brine (pH 10), twice with brine and finally with 6 M HCl (pH 2). The resulting organic layer was concentrated to dryness to afford DXM *N*-oxide hydrochloride **26** as a white powder which decomposes at temperatures above 115 °C (6.8 mmol, 84 %). IR (ATR): 3018.8 (w), 2923.5 (m-br) 2427.8 (s, OH stretch), 2379.0 (s-br), 1494.3 (s), 1443.3 (s), 1277.7 (s), 1035.3 (s), 799.5 (vs, OH bend). ¹H NMR (CDCl₃, 300 MHz) δ 7.07 (d, 1H), 6.84 (d, 1H), 6.79 (m, 1H), 4.28 (s, 1H, broad), 2.92 (m, 1H), 3.80 (s, 3H), 3.76 (s, 3H), 3.40-3.25 (m, 1H), 3.16-2.87 (m, 2H), 2.80 (m, 1H), 2.35-2.25 (m, 2H), 1.75-1.64 (m, 1H), 1.68-1.53 (m, 2H), 1.50-1.32 (m, 3H), 1.32-1.20 (m, 1H), 1.17-0.97 (m,

1H). ^{13}C NMR (CDCl_3 , 75 MHz) δ 159.69, 138.81, 129.27, 123.28, 112.49, 111.46, 72.85, 59.56, 55.34, 37.30, 36.55, 35.65, 35.09, 27.13, 25.77, 21.67. ESI-MS (+): Calcd for $\text{C}_{18}\text{H}_{26}\text{NO}_2$ m/z: 288.20. Found m/z: 288.3. Anal. Calcd for $[\text{C}_{18}\text{H}_{26}\text{NO}_2]^+\text{Cl}^-$: C, 66.75; H, 8.09; N, 4.32. Found: C, 66.82; H, 8.10; N, 4.37.

5.3. Preparation of Nanoscale Zero Valent Iron

5.3.1. Preparation of Nanoscale Zero Valent Iron for Immediate Use

The following procedure is a modified version of the procedure published by Moores *et al.*³⁴ 0.17 g (0.62 mmol) of iron(II) sulfate heptahydrate was dissolved 7 mL of water and 3 mL of methanol and stirred at 320 RPM using a mechanical stirrer in an appropriately sized 2-neck round bottom flask while a 0.12 M aqueous solution of sodium borohydride was added dropwise at a rate of 1 drop per second. After several drops had been added a black precipitate formed. The mixture of solution and black precipitate was then stirred for an additional 5 minutes before being transferred evenly into two 15 mL centrifuge tubes. Next followed the washing process which consisted of five repetitions of centrifugation (five minutes each at 3200 RPM) and decantation of the supernatant fluid. Before each centrifugation the tubes were shaken vigorously such that the iron particles were suspended in the liquid. After the initial centrifugation and decantation (washing # 1) the tubes were filled to the 5 mL mark with 3 mL of water and 2 mL of methanol (washing # 2). The same washing process was then repeated (washing # 3). Next the tubes were filled with the solvent to be used in the *N*-demethylation reaction (washing # 4). The same washing process was then repeated (washing # 5). At this point the nZVI was suspended in the appropriate solvent and was ready to be added to the *N*-demethylation reaction flask.

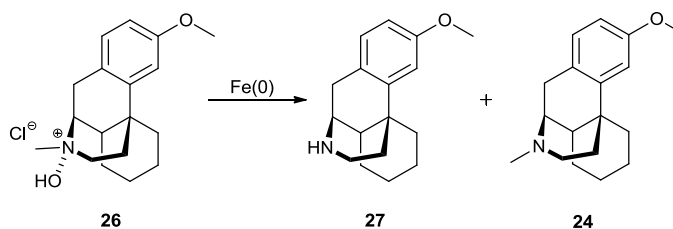
5.3.2. Preparation of nZVI for Storage

The following procedure is a modified version of the procedure published by Audrey Moores *et al.*³⁴ 0.17 g (0.62 mmol) of iron(II) sulfate heptahydrate was dissolved in 7 mL of water and 3 mL of methanol and stirred at 320 RPM using a mechanical stirrer in an appropriately sized 2-neck round bottom flask while a 0.12 M aqueous solution of sodium borohydride was added dropwise at a rate of 1 drop per second. After several drops had been added a black precipitate formed. The mixture of solution and black precipitate was then stirred for an additional 5 minutes and was then gravity filtered and washed several times with methanol to completely replace water with methanol. The nZVI was then scraped off the filter pad into a round bottom flask. Methanol was used to wash the filter pad, ensuring a maximum amount of material was transferred. The methanol was then removed using a rotary evaporator. The nZVI was transferred into a vial and stored in a desiccator.

5.4. N-demethylation of Dextromethorphan N-oxide Hydrochloride

5.4.1. N-demethylation via Iron(0) Dust – General Procedure

Figure 24. Synthesis of N-nordextromethorphan, **27**



Following a modified procedure,²⁰ 0.200 g (0.618 mmol) of DXM *N*-oxide hydrochloride, **26**, was added to 15 mL isopropyl alcohol or 10 mL of chloroform or

methanol and was stirred until all of **26** was dissolved. The specified amount of iron(0) powder was then added to the reaction flask and magnetically stirred at 900 RPM for the specified length of time. The reaction mixture was then gravity filtered and the filter paper was washed with chloroform. The filtrate and washings were combined and concentrated to dryness. The residue was then purified *via* column chromatography on SiO₂ (pore size 60 Å, particle size 220-440 mesh) using a chloroform/methanol/ammonium hydroxide gradient (85:15:1) which isolated the *N*-demethylated product, **27**. A column 20 mm in diameter filled to approximately 20 cm of height with SiO₂ was sufficient for separation of *N*-nordextromethorphan, **27**, from DXM, **24**, and other by-products. *N*-nordextromethorphan was isolated as a colorless oil (yield as per Tables 2-7). IR (ATR): 2922.0 (s), 2853.7 (m), 1608.3 (m), 1573.2 (w), 1495.1 (s), 1454.3 (m), 1400.3 (m), 1322.2 (w), 1269.8 (m), 1236.0 (vs), 1187.7 (w), 1158.7 (w), 1118.8 (w), 1066.6 (w), 1038.8 (s), 986.7 (w), 858.0 (m), 796.0 (m). ¹H NMR (CDCl₃, 300 MHz) δ 7.03 (d, 1H), 6.81 (d, 1H), 6.74 (m, 1H), 4.90 (s, 1H), 3.76 (s, 3H), 3.18-2.98 (m, 2H), 2.87-2.43 (m, 3H), 2.41-2.23 (m, 1H), 1.82-1.72 (m, 1H), 1.72-1.43 (m, 3H), 1.43-1.22 (m, 5H), 1.18-0.97 (m, 1H). ¹³C NMR (CDCl₃, 75 MHz) δ 158.31, 141.23, 129.35, 128.68, 111.21, 110.85, 55.20, 51.13, 45.05, 41.96, 38.88, 38.02, 36.78, 32.55, 26.66, 26.57, 22.05. ESI-MS (+): Calcd for C₁₇H₂₃NO m/z: 258.18 [M + H]⁺. Found m/z: 258.1 [M + H]⁺.

Dextromethorphan was isolated as a light red-brown oil. IR (ATR): 2923.8 (s), 2854.9 (m), 1663.8 (w), 1606.43 (m), 1578.8 (w), 1496.1 (s), 1452.7 (s-br), 1270.8 (m), 1237.2 (vs), 1159.2 (m), 1120.5 (w), 1037.8.7 (vs), 856.9 (m), 804.1 (m), 752.1 (s). ¹H NMR (MeOD, 300 MHz) δ 7.02 (d, 1H), 6.80 (d, 1H), 6.73 (m, 1H), 3.75 (s, 3H), 3.15-2.95 (d, 1H), 2.90-2.79 (m, 1H), 2.72-2.59 (m, 1H), 2.45-2.39 (m, 2H), 2.39-2.30 (s, 3H), 2.19-2.05 (m, 1H),

1.89-1.61 (m, 3H), 1.61-0.1.50 (m, 1H), 1.50-1.38 (m, 2H), 1.38-1.27 (m, 3H), 1.19-1.07 (m, 1H). ^{13}C NMR (CDCl_3 , 75 MHz) δ 158.2, 141.8, 129.9, 128.5, 111.1, 110.7, 58.0, 55.2, 47.3, 45.4, 42.8, 41.1, 37.3, 36.7, 26.8, 26.6, 23.4, 22.3. ESI-MS (+): Calcd for $\text{C}_{18}\text{H}_{25}\text{NO}$ m/z: 272.2 $[\text{M} + \text{H}]^+$ Found m/z: 273.3

5.4.2. *N*-demethylation via Nanoscale Zero Valent Iron

A solution of DXM *N*-oxide containing 200 mg per 15 mL of isopropyl alcohol or 5 mL of chloroform or methanol was stirred until all of the DXM *N*-oxide was dissolved. A suspension of nZVI (see sections 5.3.1 and 5.3.2) in 5 mL of isopropyl alcohol, chloroform or methanol was then added to the reaction flask and stirred at 900 RPM for the specified length of time. The remainder of the workup procedure and the characterization of *N*-nordextromethorphan and dextromethorphan follow as per section 5.4.1.

6. References

- (1) IUPAC. *Compendium of Chemical Terminology, 2nd Ed. (the "Gold Book")*; McNaught, A D; Wilkinson, A., Ed.; Oxford, 1997.
- (2) BSBI List 2007 <http://www.bsbi.org.uk/BSBIList2007.xls> (accessed Dec 17, 2016).
- (3) Miller, J W; Anderson, H. H. The Effect of N-Demethylation on Certain Pharmacologic Actions of Morphine, Codeine, and Meperidine in the Mouse. *J. Pharmacol. Exp. Ther.* **1954**, *112*, 191–196.
- (4) Axelrod, J. Possible Mechanism of Tolerance to Narcotic Drugs. *Sci. New Ser.* **1956**, *124* (3215), 263–264.
- (5) Cochin, J; Axelrod, J. The Inhibitory Action of Nalorphine on the Enzymatic N-Demethylation of Narcotic Drugs. *J. Pharmacol. Exp. Ther.* **1957**, *121*, 107–112.
- (6) C. Elison, H. Rapoport, R. L. and H. W. E. Effect of Deuteration of N-CH₃ Group on Potency and Enzymatic N-Demethylation of Morphine. **1961**, *134* (3485), 1078–1079.
- (7) Yu, H.; Prisinzano, T.; Dersch, C. M.; Marcus, J.; Rothman, R. B.; Jacobson, A. E.; Rice, K. C. Synthesis and Biological Activity of 8beta-Substituted Hydrocodone Indole and Hydromorphone Indole Derivatives. *Bioorg. Med. Chem. Lett.* **2002**, *12* (2), 165–168.
- (8) Hosztafi, S. Recent Advances in the Chemistry of Oripavine and Its Derivatives. *Adv. Biosci. Biotechnol.* **2014**, *5* (July), 704–717.
- (9) von Braun, J. No Title. *Ber. Dtsch. Chem. Ges.* **1900**, *33*, 1438.

- (10) Weijlard, J.; Erickson, A. E. No Title. *J. Am. Chem. Soc.* **1942**, *64*, 869.
- (11) Bentley, K. W.; Hardy, D. G. No Title. *J. Am. Chem. Soc.* **1967**, *89*, 3281.
- (12) Fisher Scientific; NJ, U. Cyanogen bromide; Cat No. : O6103-25; O6103-100 [Online].
- (13) A. Pohland; H. R. Sullivan, J. Normorphines. 3,342,824, 1967.
- (14) Santamaria, J.; Ouchabane, R.; Rigaudy, J. Electron-Transfer Activation. Photochemical N-Demethylation of Tertiary Amines. *Tetrahedron Lett.* **1989**, *30* (22), 2927–2928.
- (15) Ripper, J. A.; Tiekink, R. T.; Scammells, P. J. Photochemical N -Demethylation of Alkaloids. **2001**, *11*, 443–445.
- (16) Santamaria, J.; Ouchabane, R.; Rigaudy, J. Electron-Transfer Activation. Salt Effects on the Photooxidation of Tertiary Amines: A Useful N-Demethylation Method. *Tetrahedron Lett.* **1989**, *30* (30), 3977–3980.
- (17) Lindner, J. H. E.; Kuhn, H. J.; Gollnick, K. Demethylation of Codeine to Norcodeine by Sensitized Photooxidation. *Tetrahedron Lett.* **1972**, No. 17, 1705.
- (18) Polonovski, M.; Polonovski, M. No Title. *Bull. Soc. Chim. Fr.* **1927**, *41*, 1190–1208.
- (19) McCamley, K.; Ripper, J. A.; Singer, R. D.; Scammells, P. J. Efficient N-Demethylation of Opiate Alkaloids Using a Modified Nonclassical Polonovski Reaction. *J. Org. Chem.* **2003**, *68* (25), 9847–9850.
- (20) Kok, G. B.; Pye, C. C.; Singer, R. D.; Scammells, P. J. Two-Step iron(0)-Mediated N-Demethylation of N -Methyl Alkaloids. *J. Org. Chem.* **2010**, *75* (14), 4806–4811.

- (21) Davis, Mark E., Davis, R. J. *Fundamentals of Chemical Reaction Engineering*; McGraw-Hill Higher Education: New York, 2003.
- (22) Moshfegh, a Z. Nanoparticle Catalysts. *J. Phys. D. Appl. Phys.* **2009**, *42* (23), 233001.
- (23) Ghadiri, M. R.; Granja, J. R.; Milligan, R. A.; McRee, D. E.; Khazanovich, N. Self-Assembling Organic Nanotubes Based on a Cyclic Peptide Architecture. *Nature* **1993**, *366* (6453), 324–327.
- (24) BUSSER, G. W.; VANOMMEN, J. G. CATALYSIS WITH POLYMER-SUPPORTED NANOSCALE RHODIUM PARTICLES. *Abstr. Pap. Am. Chem. Soc.* **1995**, *209* (2), 53 – PETR.
- (25) Vitulli, G.; Pitzalis, E.; Verrazzani, A.; Pertici, P.; Salvadori, P.; Martra, G. Nanoscale Pt Powders Derived from Solvated Pt Atoms in Catalysis. In *Synthesis and properties of mechanically alloyed and nanocrystalline materials, pts 1 and 2*; M, F. D. and M., Ed.; Materials Science Forum; TRANS TECH PUBLICATIONS LTD: LAUBLSRUTISTR 24, CH-8717 STAFA-ZURICH, SWITZERLAND, 1997; Vol. 235-2, pp 929–934.
- (26) Toshima, N.; Yonezawa, T. Bimetallic Nanoparticles - Novel Materials for Chemical and Physical Applications. *NEW J. Chem.* **1998**, *22* (11), 1179–1201.
- (27) Bell, A. T. The Impact of Nanoscience on Heterogeneous Catalysis. **2003**, *299* (March), 1688–1692.
- (28) Dey, R.; Mukherjee, N.; Ahammed, S.; Ranu, B. C. Highly Selective Reduction of Nitroarenes by iron(0) Nanoparticles in Water. *Chem. Commun.* **2012**, *48* (64),

7982–7984.

- (29) Sonnenberg, J. F.; Coombs, N.; Dube, P. A.; Morris, R. H. Iron Nanoparticles Catalyzing the Asymmetric Transfer Hydrogenation of Ketones. *J. Am. Chem. Soc.* **2012**, *134* (13), 5893–5899.
- (30) Kelsen, V.; Wendt, B.; Werkmeister, S.; Junge, K.; Beller, M.; Chaudret, B. The Use of Ultrasmall iron(0) Nanoparticles as Catalysts for the Selective Hydrogenation of Unsaturated C-C Bonds. *Chem. Commun.* **2013**, *49* (33), 3416–3418.
- (31) Kanel, S. R.; Manning, B.; Charlet, L.; Choi, H. Removal of Arsenic (III) from Groundwater by Nanoscale Zero-Valent Iron. *Environ. Sci. Technol.* **2005**, *39* (5), 1291–1298.
- (32) Li, X. Q.; Cao, J.; Zhang, W. X. Stoichiometry of Cr(VI) Immobilization Using Nanoscale Zero Valent Iron (nZVI): A Study with High-Resolution X-Ray Photoelectron Spectroscopy (HR-XPS). *Ind. Eng. Chem. Res.* **2008**, *47* (7), 2131–2139.
- (33) Li, Z.; Greden, K.; Alvarez, P. J. J.; Gregory, K. B.; Lowry, G. V. Adsorbed Polymer and NOM Limits Adhesion and Toxicity of Nano Scale Zerovalent Iron to E. Coli. *Environ. Sci. Technol.* **2010**, *44* (9), 3462–3467.
- (34) Cirtiu, C. M.; Raychoudhury, T.; Ghoshal, S.; Moores, A. Systematic Comparison of the Size, Surface Characteristics and Colloidal Stability of Zero Valent Iron Nanoparticles Pre- and Post-Grafted with Common Polymers. *Colloids Surfaces A Physicochem. Eng. Asp.* **2011**, *390* (1-3), 95–104.
- (35) Han, Y.; Yang, M. D. Y.; Zhang, W.; Yan, W. Optimizing Synthesis Conditions of

- Nanoscale Zero-Valent Iron (nZVI) through Aqueous Reactivity Assessment. *Front. Environ. Sci. Eng.* **2015**, *9* (5), 813–822.
- (36) Zhu, S.-N.; Liu, G.; Hui, K. S.; Ye, Z.; Hui, K. N. A Facile Approach for the Synthesis of Stable Amorphous Nanoscale Zero-Valent Iron Particles. *Electron. Mater. Lett.* **2014**, *10* (1), 143–146.
- (37) Liu, Y.; Majetich, S. A.; Sholl, D. S. TCE Dechlorination Rates , Pathways , and Efficiency of Nanoscale Iron Particles with Different Properties. **2005**, *39* (5), 1338–1345.
- (38) Petala, E.; Dimos, K.; Douvalis, A.; Bakas, T.; Tucek, J.; Zbořil, R.; Karakassides, M. A. Nanoscale Zero-Valent Iron Supported on Mesoporous Silica: Characterization and Reactivity for Cr(VI) Removal from Aqueous Solution. *J. Hazard. Mater.* **2013**, *261*, 295–306.
- (39) Martin, J. E.; Herzing, A.; Yan, W.; Li, X.; Koel, B. E.; Kiely, C. J.; Zhang, W. Determination of the Oxide Layer Thickness in Core-Shell Zerovalent Iron Nanoparticles. *Langmuir* **2008**, *24* (8), 4329–4334.
- (40) Raveendran, P.; Fu, J.; Wallen, S. L. Completely “Green” Synthesis and Stabilization of Metal Nanoparticles. *J. Am. Chem. Soc.* **2003**, *125* (46), 13940–13941.
- (41) Kauffeldt, Th.; Lakne, H.; Lohmann, M.; Schmidt-Ott, A. Nanocharacterization of Small Particles Produced in a Gas. *Nanostructured Mater.* **1995**, *6* (1-4), 365–368.
- (42) Nurmi, J. T.; Tratnyek, P. G.; Sarathy, V.; Baer, D. R.; Amonette, J. E.; Pecher, K.; Wang, C.; Linehan, J. C.; Matson, D. W.; Penn, R. L.; et al. Characterization and

Properties of Metallic Iron Nanoparticles: Spectroscopy, Electrochemistry, and Kinetics. *Environ. Sci. Technol.* **2005**, *39* (5), 1221–1230.

- (43) Synthesis, B. R.; Wang, Q.; Snyder, S.; Kim, J.; Choi, H. Aqueous Ethanol Modified Nanoscale Zerovalent Iron in Aqueous Ethanol Modified Nanoscale Zerovalent Iron in Bromate Reduction : Synthesis , Characterization , and Reactivity. *Environ. Sci. Technol* **2009**, *43* (9), 3292–3299.
- (44) Shih, Y. hsin; Tai, Y. tsung. Reaction of Decabrominated Diphenyl Ether by Zerovalent Iron Nanoparticles. *Chemosphere* **2010**, *78* (10), 1200–1206.
- (45) Majumdar, K. C.; Chattopadhyay, B.; Chakravorty, S.; Pal, N.; Sinha, R. K. A New Type of Symmetrical Banana-Shaped Material Based on N-Methyldiphenylamine as a Core Moiety Exhibiting an Ad² Transition. *Tetrahedron Lett.* **2008**, *49* (50), 7149–7152.
- (46) Phenrat, T.; Saleh, N.; Sirk, K.; Tilton, R. D.; Lowry, G. V. Aggregation and Sedimentation of Aqueous Nanoscale Zerovalent Iron Dispersions. *Environ. Sci. Technol.* **2007**, *41* (1), 284–290.
- (47) Dong, Z.; Scammells, P. J. New Methodology for the N-Demethylation of Opiate Alkaloids. *J. Org. Chem.* **2007**, *72* (26), 9881–9885.
- (48) Bolcskei, H.; Mak, M.; Dravec, F.; Domany, G. Synthesis of Deuterated Dextromethorphan Derivatives. *Arkivoc* **2008**, *2008* (3), 182–193.
- (49) Shi, L. na; Zhang, X.; Chen, Z. liang. Removal of Chromium (VI) from Wastewater Using Bentonite-Supported Nanoscale Zero-Valent Iron. *Water Res.* **2011**, *45* (2), 886–892.

- (50) Chastanet, J.; Roussi, G. N-Methylpiperidine N-Oxide as a Source of Nonstabilized Ylide: A New and Efficient Route to Octahydroindolizine Derivatives. *J. Org. Chem.* **1985**, *50* (16), 2910–2914.
- (51) *Science of Synthesis : Houben-Weyl Methods of Molecular Transformations*; Banert, K.; Drabowicz, J.; Oestreich, M.; Plietker, B. J.; Schaumann, E.; Stoltz, B. M.; Weinreb, S. M., Ed.; Stuttgart: New York, 2013.
- (52) *Science of Synthesis : Houben-Weyl Methods of Molecular Transformations*; Banert, K.; Drabowicz, J.; Oestreich, M.; Plietker, B. J.; Schaumann, E.; Stoltz, B. M.; Weinreb, S. M., Ed.; Stuttgart: New York, 2013.
- (53) Li, Y.; Zhang, Y.; Li, J.; Zheng, X. Enhanced Removal of Pentachlorophenol by a Novel Composite: Nanoscale Zero Valent Iron Immobilized on Organobentonite. *Environ. Pollut.* **2011**, *159* (12), 3744–3749.